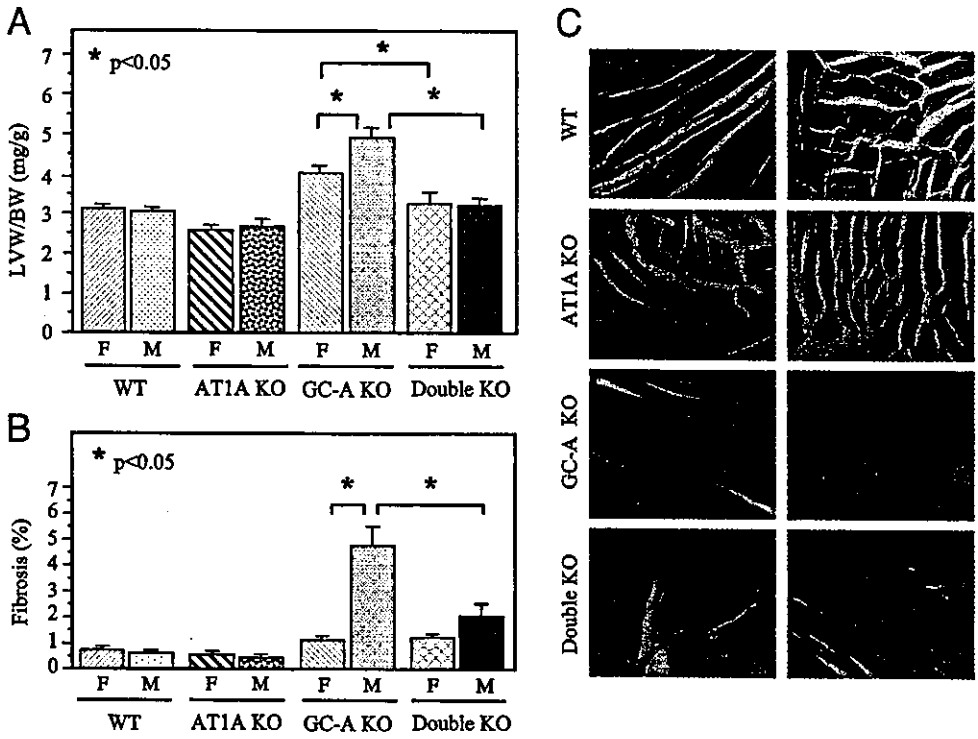

FIG. 5. Deletion of the AT1A receptor gene abolishes the gender-related differences in LVW/BW (A) and the relative levels of left ventricular fibrosis (B). C, Representative photomicrographs demonstrating fibrosis (red) in GC-A KO mice. Animals were analyzed at 16 wk of age. Values are mean ± SEM; n = 5–9 per group; *, $P < 0.05$.

this effect (12). Like cardiac geometric changes, changes in ANP and BNP, or markers for ventricular fibrosis, collagen I, and collagen III were higher in male GC-A KO mice than in females and were reduced by removal of testes. These findings suggest that androgens play an important role in gender-related cardiac differences in GC-A KO mice. Castration in males and AR antagonist could not reduce the cardiac mass and fibrosis to WT levels, suggesting that more than androgens are involved.

Ang II is known to potently stimulate cardiomyocyte and fibroblast growth, both *in vitro* and *in vivo* (31, 32), and the tissue renin-Ang system is known to play a key role in cardiac remodeling (33). It has been proposed that increased ACE abundance in the hypertrophied and failing heart may contribute to the local generation of Ang II and impact cardiac remodeling through local paracrine or autocrine effects (34–36). The greater abundance of ventricular ACE in males may contribute to the tendency of male rodents to develop cardiac abnormalities, which has been described in transgenic mouse models (37, 38) and spontaneously hypertensive rats (39) and in response to left ventricular pressure overload in rats (10) and in humans (40–42). It has been reported that hepatic Agt mRNA levels are higher in intact male hypertensive rats than in the females; moreover, those levels are reduced by orchidectomy and increased by administration of testosterone (43). Recently, Freshour *et al.* (44) demonstrated a gender difference in the expression of ACE in the murine heart with greater cardiac ACE levels seen in male animals compared with females. Moreover, ventricular ACE levels were substantially decreased in androgen-deprived males (44). Consistent with those reports, our data show that levels of cardiac Agt and ACE expression are higher in the ventricles of both GC-A KO and WT males than they are in females. Castration reduced expression of Agt in the male ventricle to levels approximating those seen in the females in both WT and GC-A KO mice. Given the evidence that Ang II has hypertrophic and fibrogenic activities in the heart, Ang II is a possible candidate to link androgens with cardiac abnormalities. It should be noted, however, that gender-related increases in LVW/BW ratios and interstitial fibrosis were observed only in the GC-A KO mice but not in WT mice, despite the similar up-regulation of Agt and ACE expression in ventricles of both genotypes of mice. We recently observed that GC-A signaling counteracts Ang II-induced cardiac abnormalities. A subpressor dose of Ang II increased cardiac mass and fibrosis only in male GC-A KO but not WT mice, suggesting an augmented responsiveness to Ang II in the heart of GC-A KO mice (22). Thus, we speculate that gender-related differences in the heart were made manifest by lacking inhibitory actions of GC-A on AT1 signaling in GC-A KO mice. Inhibitory effects of GC-A were also supported by the overexpression of TGF-β1 and -β3, which are activated by AT1A signaling and responsible for interstitial fibrosis (28, 45–47), in GC-A KO mice.

To further test this hypothesis, we deleted the AT1A receptor gene, which mediates classical Ang II actions, including cardiac hypertrophy and fibrosis, by crossing GC-A KO mice and AT1A KO mice. The gender-related cardiac differences were absent in the double-KO mice. Furthermore, castration of males did not reduce and testosterone administration failed to increase the cardiac mass and fibrosis in male double-KO mice. These results strongly suggest that GC-A prevents androgen-induced cardiac abnormalities mainly by inhibiting the androgen-Ang II-AT1A axis.

The present data did not indicate that androgens and Ang II solely provide a causative contribution to gender-related cardiac differences in GC-A KO mice. LVW/BW in male GC-A KO mice after castration or flutamide treatment were

comparable to that in female GC-A KO mice, but the degree of fibrosis was still higher in male GC-A KO mice after the treatments than in females, suggesting androgens mostly contribute to gender-related left ventricular hypertrophy, and at least approximately 50% to the gender-related increase in fibrosis. In the case of AT1A blockade, LVW/BW in GC-A KO mice were reduced to the level corresponding to that in WT mice, in which there was no difference in hypertrophy, and fibrosis was more intensively reduced by knocking out the AT1A receptor, compared with blockade of ARs. These findings suggest that AT1A signaling contributes not only to gender-related cardiac abnormalities but also to abnormalities specifically observed in both genders of GC-A KO mice, suggesting androgen is one of the factors up-regulating the Ang system. Additional studies are required to elucidate the entire mechanism for gender-related difference observed in GC-A KO mice, in which other molecules, such as catecholamines and endothelin, would be involved.

Another interesting finding is that castration or the treatment with androgen antagonist improved cardiac abnormalities in GC-A KO mice without significant change in SBP. As mentioned above, a subpressor dose of Ang II exaggerated hypertrophy and fibrosis in GC-A KO mice (22). It is likely, therefore, that androgen-induced Ang II is sufficient for inducing hypertrophy and fibrosis in GC-A KO mice but not to elevate BP.

The presence or absence of androgens in male GC-A KO mice showed marked effects on the expression levels of ANP. The molecular mechanism is unclear at present. In the present study, despite the similar up-regulation of Agt and ACE expression in ventricles of both male WT and GC-A KO mice, ANP was markedly increased only in male GC-A KO mice. We demonstrated a similar expression level of AT1A mRNA in males and females of both WT and GC-A KO mice (data not shown). Therefore, it seems that androgen-induced intracellular signaling at a postreceptor level for modulation of ANP gene expression is up-regulated in GC-A KO mice. Ang II is known to increase ANP expression mediated by protein kinase C or MAPK (48). Further examination is necessary to determine whether the protein kinase C or MAPK pathway is involved in the elevation of ANP by androgens.

Recently, Nakayama *et al.* (49) described a functional mutation in the 5′-flanking region of the human GC-A gene that reduces transcriptional activity by more than 70% in reporter gene assay, is present in approximately 5% of the hypertensive individuals in Japan, and is associated with cardiac hypertrophy. Evidence also suggests that GC-A receptors may be down-regulated in patients with chronic, severe heart failure (50). Indeed, there may be substantial numbers of patients whose abnormal GC-A signaling makes them susceptible to androgen-induced cardiac abnormalities. From the clinical points of view, the present study raises the possibility of the prophylactic use of Ang II receptor blocker or AR antagonist in patients with loss of functional mutations in the GC-A gene.

Taken together, our findings strongly support the hypothesis that androgen contributes to cardiac abnormalities *via* the AT1A receptor. Furthermore, this androgenic effect is normally inhibited by stimulation of GC-A by natriuretic peptides.

Acknowledgments

We thank Ms. Makoto Mukai and Ms. Itone Makino for their excellent secretarial assistance and Ms. Mika Inoue for her technical assistance. Dr. Yuhao Li is a foreign research fellow of the Japan Society for the Promotion of Science.

Received June 30, 2003. Accepted October 22, 2003.

Address all correspondence and requests for reprints to: Yoshihiko Saito, First Department of Internal Medicine, Nara Medical University, 840, Shijo-cho, Kashihara, Nara 634-8522, Japan. E-mail: yssaito@naramed-u.ac.jp.

This work was supported in part by research grants from Japanese Ministry of Education, Science and Culture, the Japanese Ministry of Health and Welfare, the Japanese Society for the Promotion of Science Research for the Future program (JSPS-RFTF96I00204 and JSPS-RFTF98L00801), the Uehara Memorial Foundation, the Smoking Research Foundation, and the Howard Hughes Medical Institute.

References

1. **Devereux RB, Pickering TG, Alderman MH, Chien S, Borer JS, Laragh JH** 1987 Left ventricular hypertrophy in hypertension: prevalence and relationship to pathophysiologic variables. Hypertension 9(Suppl II):53–60
2. **Kaplinsky E** 1994 Significance of left ventricular hypertrophy in cardiovascular morbidity and mortality. Cardiovasc Drugs Ther 8:549–556
3. **Neyses L, Pelzer T** 1995 The biological cascade leading to cardiac hypertrophy. Eur Heart J 16(Suppl N):8–11
4. **Weber KT, Brilla CG** 1991 Pathological hypertrophy and cardiac interstitium. Fibrosis and renin-angiotensin-aldosterone system. Circulation 83:1849–1865
5. **Hayward CS, Kelly RP, Collins P** 2000 The roles of gender, the menopause and hormone replacement on cardiovascular function. Cardiovasc Res 46: 28–49
6. **Fiebach NH, Viscoli CM, Horwitz RI** 1990 Differences between women and men in survival after myocardial infarction. JAMA 263:1092–1096
7. **de Simone G, Devereux RB, Daniels SR, Meyer RA** 1995 Gender differences in ventricular growth. Hypertension 26:979–983
8. **Luchner A, Brockel U, Muscholl M, Hense HW, Doring A, Riegger GA, Schunkert H** 2002 Gender-specific differences of cardiac remodeling in subjects with left ventricular dysfunction: a population-based study. Cardiovasc Res 53:720–727
9. **Crabbe DL, Dipla K, Ambati S, Zafeiridis A, Gaughan JP, Houser SR, Margulies KB** 2003 Gender differences in post-infarction hypertrophy in end-stage failing hearts. J Am Coll Cardiol 41:300–306
10. **Weinberg EO, Thienelt CD, Katz SE, Bartunek J, Tajima M, Rohrbach S, Douglas PS, Lorell BH** 1999 Gender differences in molecular remodeling in pressure overload hypertrophy. J Am Coll Cardiol 34:264–273
11. **Meyer R, Linz KW, Surges R, Meinardus S, Vees J, Hoffmann A, Windholz O, Grohe C** 1998 Rapid modulation of L-type calcium current by acutely applied oestrogens in isolated cardiac myocytes from human, guinea-pig and rat. Exp Physiol 83:305–321
12. **Marsh JD, Lehmann MH, Ritchie RH, Gwathmey JK, Green GE, Schiebinger RJ** 1998 Androgen receptors mediate hypertrophy in cardiac myocytes. Circulation 98:256–261
13. **Dubey RK, Gillespie DC, Jackson EK, Keller PJ** 1998 17β-Estradiol, its metabolites, and progesterone inhibit cardiac fibroblast growth. Hypertension 31:522–528
14. **Chen SJ, Li H, Durand J, Oparil S, Chen YF** 1996 estrogen reduces myointimal proliferation after balloon injury of rat carotid artery. Circulation 93:577–584
15. **Somjen D, Kohen F, Jaffe A, Amir-Zaltsman Y, Knoll E, Stern N** 1998 Effect of gonadal steroids and their antagonists on DNA synthesis in human vascular cells. Hypertension 32:39–45
16. **Fujimoto R, Morimoto I, Morita E, Sugimoto H, Ito Y, Eto S** 1994 Androgen receptors, 5α-reductase activity and androgen-dependent proliferation of vascular smooth muscle cells. J Steroid Biochem Mol Biol 50:169–174
17. **Cabral AM, Vasquez EC, Moyses MR, Antonio A** 1988 Sex hormone modulation of ventricular hypertrophy in sinoaortic denervated rats. Hypertension 11:193–197
18. **Malhotra A, Buttrick P, Scheuer J** 1990 Effects of sex hormones on development of physiological and pathological cardiac hypertrophy in male and female rats. Am J Physiol 259:H866–H871
19. **Lopez MJ, Wong SK, Kishimoto I, Dubois S, Mach V, Friesen J, Garbers DL, Beuve A** 1995 Salt-resistant hypertension in mice lacking the guanylyl cyclase-A receptor for atrial natriuretic peptide. Nature 378:65–68
20. **Oliver PM, Fox JE, Kim R, Rockman HA, Kim HS, Reddick RL, Pandey KN, Milgram SL, Smithies O, Maeda N** 1997 Hypertension, cardiac hypertrophy, and sudden death in mice lacking natriuretic peptide receptor A. Proc Natl Acad Sci USA 94:14731–14735
21. **Sugaya T, Nishimatsu S, Tanimoto K, Takimoto E, Yamagishi T, Imamura K, Goto S, Imaizumi K, Hisada Y, Otsuka A, Uchida H, Sugiura M, Fukuta**

K, Fukamizu A, Murakami K 1995 Angiotensin II type 1a receptor-deficient mice with hypotension and hyperreninemia. J Biol Chem 270:18719–18722
22. Li Y, Kishimoto I, Saito Y, Harada M, Kuwahara K, Izumi T, Takahashi N, Kawakami R, Tanimoto K, Nakagawa Y, Nakanishi M, Adachi Y, Garbers DL, Fukamizu A, Nakao K 2002 Guanylyl cyclase-A inhibits angiotensin II type 1A receptor-mediated cardiac remodeling, an endogenous protective mechanism in the heart. Circulation 106:1722–1728
23. Labrie F 1993 Mechanisms of action and pure antiandrogenic properties of flutamide. Cancer 72:3816–3827
24. Reckelhoff JF, Zhang H, Srivastava K, Granger JP 1999 Gender differences in hypertension in spontaneously hypertensive rats: role of androgens and androgen receptor. Hypertension 34:920–923
25. Mendelsohn ME, Karas RH 1999 The protective effects of estrogen on the cardiovascular system. N Engl J Med 340:1801–1811
26. van Eickels M, Grohe C, Cleutjens JP, Janssen BJ, Wellens HJ, Doevendans PA 2001 17β-Estradiol attenuates the development of pressure-overload hypertrophy. Circulation 104:1419–1423
27. Farnsworth NR, Bingel AS, Cordell GA, Crane FA, Fong HHS 1975 Potential value of plants as sources of new antifertility agents. J Pharm Sci 64:717–754
28. Price KR, Fenwick GR 1985 Naturally occurring oestrogens in foods: a review. Food Addit Contam 2:73–106
29. Degen GH, Janning P, Diel P, Bolt HM 2002 Estrogenic isoflavones in rodent diets. Toxicol Lett 128:145–157
30. Mcgill HC, Sheridan PJ 1981 Nuclear uptake of sex steroid hormones in the cardiovascular system of the baboon. Circ Res 48:238–244
31. Sadoshima J, Izumo S 1993 Molecular characterization of angiotensin II-induced hypertrophy of cardiac myocytes and hyperplasia of cardiac fibroblasts. Critical role of AT1 receptor subtype. Circ Res 73:413–423
32. Schorb W, Booz GW, Dostal DE, Conrad KM, Chang KC, Baker KM 1993 Angiotensin II is mitogenic in neonatal rat cardiac fibroblasts. Circ Res 72: 1245–1254
33. McDonald KM, Garr M, Carlyle PF, Francis GS, Hauer K, Hunter DW, Parish T, Stillman A, Cohn JN 1999 Relative effects of α1-adrenergic blockade, converting enzyme inhibitor therapy, and angiotensin II subtype 1 receptor blockade on ventricular remodeling in the dog. Circulation 90:3034–3046
34. Bader M, Peters J, Baltatu O, Muller DN, Luft FC, Ganten D 2001 Tissue rennin-angiotensin systems: new insights from experimental animal models in hypertensive research. J Mol Med 79:76–102
35. Pratt RE 1999 Angiotensin II and the control of cardiovascular structure. J Am Soc Nephrol 10:S120–S128
36. Weber KT 1997 Extra cellular matrix remodeling in heart failure. A role for de novo angiotensin II generation. Circulation 96:4065–4082
37. Kadokami T, McTiernan CF, Kubota T, Frye CS, Feldman AM 2000 Sex-related survival differences in murine cardiomyopathy are associated with differences in TNF-receptor expression. J Clin Invest 106:589–597
38. Vikstrom KL, Factor SM, Leinwand LA 1996 Mice expressing mutant myosin are a model for hypertrophic cardiomyopathy. Mol Med 2:556–567
39. Wallen WJ, Cserti C, Belanger MP, Wittnich C 2000 Gender-differences in myocardial adaptation to afterload in normotensive and hypertensive rats. Hypertension 36:774–779
40. Carroll JD, Carroll EP, Feldman T, Ward DM, Lang RM, McGaughey D, Karp RB 1992 Sex-associated differences in left ventricular function in aortic stenosis of the elderly. Circulation 86:1099–1107
41. Douglas PS, Katz SE, Weinberg EO, Chen MH, Bishop SP, Lorell BH 1998 Hypertrophic remodeling: gender differences in the early response to left ventricular pressure overload. J Am Coll Cardiol 32:1118–1125
42. Villarreal FJ, Dillmann WH 1992 Cardiac hypertrophy-induced changes in mRNA levels for TGF-β1, fibronectin, and collagen. Am J Physiol Heart Circ Physiol 262:H1861–H1866
43. Chen YF, Naftilan AJ, Oparil S 1992 Androgen-dependent angiotensinogen and renin messenger RNA expression in hypertensive rats. Hypertension 19:456–463
44. Freshour JR, Chase SE, Vikstrom KL 2002 Gender differences in cardiac ACE expression are normalized in androgen-deprived male mice. Am J Physiol Heart Circ Physiol 283:H1997–H2003
45. Border WA, Nobel NA 1994 Transforming growth factor-β in tissue fibrosis. N Engl J Med 331:1286–1292
46. Kagami S, Border WA, Miller DE, Noble NA 1994 Angiotensin II stimulates extracellular matrix protein synthesis through induction of transforming growth factor-β expression in rat glomerular mesangial cells. J Clin Invest 93:2431–2437
47. Johnston CI, Hodsman PG, Kohzuki M, Casley DJ, Fabris B, Phillips PA 1989 Interaction between atrial natriuretic peptide and the renin angiotensin aldosterone system. Am J Med 87:24S–28S
48. Sadoshima J, Izumo S 1997 The cellular and molecular response of cardiac myocytes to mechanical stress. Annu Rev Physiol 59:551–571
49. Nakayama T, Soma M, Takahashi Y, Rehemudula D, Kanmatsuse K, Furuya K 2000 Functional deletion mutation of the 5′-flanking region of type A human natriuretic peptide receptor gene and its association with essential hypertension and left ventricular hypertrophy in the Japanese. Circ Res 86:841–845
50. Tsutamoto T, Kanamori T, Morigami N, Sugimoto Y, Yamaoka O, Kinoshita M 1993 Possibility of down-regulation of atrial natriuretic peptide receptor coupled to guanylate cyclase in peripheral vascular beds of patients with chronic severe heart failure. Circulation 88:811–813

***Endocrinology* is published monthly by The Endocrine Society (http://www.endo-society.org), the foremost professional society serving the endocrine community.**

Original Article

Angiotensin II-Induced Ventricular Hypertrophy and Extracellular Signal-Regulated Kinase Activation Are Suppressed in Mice Overexpressing Brain Natriuretic Peptide in Circulation

Nobuki TAKAHASHI, Yoshihiko SAITO, Koichiro KUWAHARA, Masaki HARADA, Ichiro KISHIMOTO, Yoshihiro OGAWA, Rika KAWAKAMI, Yasuaki NAKAGAWA, Michio NAKANISHI, and Kazuwa NAKAO

Atrial and brain (B-type) natriuretic peptides (ANP and BNP, respectively) are known to exert various cardioprotective effects. For instance, knocking out the expression of ANP, BNP, or their receptor, guanylyl cyclase-A, induces cardiac hypertrophy and/or fibrosis. The cardiac effects of elevated circulating natriuretic peptides are less well understood, however. We therefore compared angiotensin (Ang) II-induced cardiac hypertrophy and fibrosis in BNP-transgenic (Tg) mice, in which circulating BNP levels were elevated by increased secretion from the liver, and their non-Tg littermates. Left ventricular expression of Ang II type 1a receptor was similar in BNP-Tg and non-Tg mice, and there was no significant difference in the elevation of blood pressure elicited by chronic infusion or acute injection of Ang II. Nevertheless, cardiac hypertrophy and fibrosis were significantly diminished in BNP-Tg mice chronically infused with Ang II. In addition, ventricular activation of extracellular signal-regulated kinase (ERK) induced by acute injection of Ang II was also diminished in BNP-Tg mice, as was activation of ERK kinase (MEK). Conversely, expression of mitogen-activated protein kinase phosphatase (MKP) was significantly increased in the ventricles of BNP-Tg mice. Based on these findings, we conclude that elevated circulating BNP exerts cardioprotective effects *via* inhibition of a ventricular ERK pathway. The mechanism responsible for this inhibition likely involves 1) increased ventricular MKP expression and 2) inhibition of transduction mediators situated upstream of ERK. (*Hypertens Res* 2003; 26: 847–853)

***Key Words*: natriuretic peptide, cardiac hypertrophy, extracellular signal-regulated kinase, angiotensin II, transgenic mice**

Introduction

For the past several years, atrial and brain (B-type) natriuretic peptide (ANP and BNP, respectively) have been used in the treatment of congestive heart failure (CHF) because their systemic infusion elicits such beneficial hemodynamic changes as arterial and venous dilatation, enhanced sodium

From the Department of Medicine and Clinical Science, Kyoto University Graduate School of Medicine, Kyoto, Japan.

This work was supported in part by Grants-in-Aid for Scientific Research from the Japanese Ministry of Education, Culture, Sports, Science and Technology, and by grants from the Japanese Ministry of Health, Labor and Welfare and the Research for the Future Program of the Japan Society for the Promotion of Science (JSPS-RFTF96I00204 and 98L00801), and by grants from the Japanese Cardiovascular Research Foundation, the Uehara Memorial Foundation, and the Smoking Research Foundation.

Address for Reprints: Yoshihiko Saito, M.D., First Department of Internal Medicine, Nara Medical University, 840 Shijo-cho, Kashihara 634–8522, Japan. E-mail: yssaito@nmu-gw.naramed-u.ac.jp

Received March 24, 2003; Accepted in revised form June 16, 2003.

excretion, and suppression of the renin-angiotensin (Ang)-aldosterone and sympathetic nervous systems (*1–6*). That is to say, natriuretic peptides (NPs) act in the body to counteract the activity of the renin-Ang system. In that regard, the well documented (*7*) benefits of angiotensin converting enzyme (ACE) inhibition in hypertension, after myocardial infarction, and in CHF suggest that NPs might be expected to exert similar cardioprotective effects. Indeed, knocking out ANP, BNP, or their receptor, guanylyl cyclase-A (GC-A; NPR-A), is known to elicit cardiac hypertrophy and/or cardiac fibrosis (*8–10*). Moreover, we have recently demonstrated and characterized the crosstalk between GC-A signaling and Ang II type 1 (AT1) receptor signaling (*11*). By contrast, neither the direct cardiac effects of elevated circulating NPs nor the molecular mechanism of the crosstalk between the NP system and Ang II system are well understood. In the present study, therefore, we used BNP-transgenic (Tg) mice, which overexpress BNP in the liver and maintain a high level of circulating BNP, to examine the effects of elevated circulating BNP on Ang II-induced cardiac hypertrophy and fibrosis. Upon confirming that increased BNP expression has cardioprotective effects, we investigated as a possible mechanism the effects of BNP on the signaling pathway *via* an extracellular signal-regulated kinase (ERK) that is activated by Ang II.

Methods

Animals

Generation of BNP-Tg mice under the control of the human serum amyloid P component promoter, which is active only in the liver after birth, was performed as described previously (*12*). Tg mice overexpressing BNP may exhibit skeletal abnormalities of variable severity, depending on the plasma BNP concentration (*13*), and thoracocyrtosis resulting from enlargement of the vertebral bodies can affect cardiovascular function. In this study, therefore, we used a BNP-Tg line carrying about 20 copies of the transgene but exhibiting no apparent thoracocyrtosis. Their responses were compared to those of their non-Tg (control) littermates. All mice were 10 weeks old and male. BNP-Tg mice exhibited elevated circulating BNP levels due to BNP secretion from the liver: at 10 weeks of age, plasma BNP concentrations were about 2 pmol/ml in the BNP-Tg mice and <0.16 pmol/ml in the non-Tg control mice. All experimental procedures were performed in accordance with the guidelines of the Animal Research Committee, Graduate School of Medicine, Kyoto University.

Materials

Synthetic Ang II was purchased from Sigma (St. Louis, USA). Anti-Ang II type-1a receptor (AT1a) antibody was a gift from Dr. Hiromi Rakugi, Osaka University Medical School, Osaka, Japan. Anti-p44/42 mitogen-activated protein kinase (MAPK, ERK1/2), anti-phospho-ERK1/2 (Thr202/Tyr204), anti-MAPK kinase (MEK1/2), and anti-phospho-MEK1/2 (Ser217/221) antibodies were from Cell Signaling Technology (Beverly, USA); anti-MAPK phosphatase (MKP)-1 antibody was from Santa Cruz Biotechnology (Santa Cruz, USA); and anti-MKP-2 antibody was from Transduction Laboratories (Lexington, USA).

Chronic Ang II Infusion

Ang II (dissolved in 0.01 mol/l acetic acid) was subcutaneously infused at the rate of 0.6 mg/kg/day for 2 weeks using an osmotic minipump (Alzet model 2002; Alza Corp., Mountain View, USA) implanted in each mouse. After 1 week of Ang II infusion, systolic blood pressure (SBP) was measured in conscious mice using a noninvasive computerized tail-cuff method (BP-98A; Softron Corp., Tokyo, Japan).

Determination of Heart Weights and Interstitial Fibrosis

After infusing Ang II for 2 weeks, the weight of the whole heart (HW) was measured, and the ratio of HW to the body weights (HW/BW) was calculated and used as an index of cardiac hypertrophy. The left ventricles were then fixed in 10% formaldehyde and prepared for routine histology. To determine the degree of collagen fiber accumulation, we randomly selected 20 fields in three individual sections and calculated the ratio of the areas of van Gieson-stained interstitial fibrosis to the total left ventricular area using a KS400 image system (Zeiss, Oberkochen, Germany). Perivascular fibrosis was excluded in the present study.

Acute Ang II Injection

Mice were anesthetized by i.p. injection of sodium pentobarbital (75 mg/kg), after which polyethylene tubing (PE 10) was inserted into the right carotid artery and the left jugular vein. Arterial blood pressure was recorded continuously from the carotid artery using a polygraph system (Fukuda Denshi, Tokyo, Japan). Once the baseline had stabilized, Ang II (0–3.0 mg/kg) was injected over a period of 1 min *via* the jugular vein.

Protein Extraction and Western Blot Analysis

Frozen ventricles were homogenized on ice in cell lysis buffer (Cell Signaling Technology), and Western blot analysis was performed as previously described (*14*).

RNA Extraction and Northern Blot Analysis

Total RNA for Northern blots was extracted from frozen ventricles by the acid guanidinium phenol chloroform method. Northern blot analysis for AT1a and c-*fos* was per-

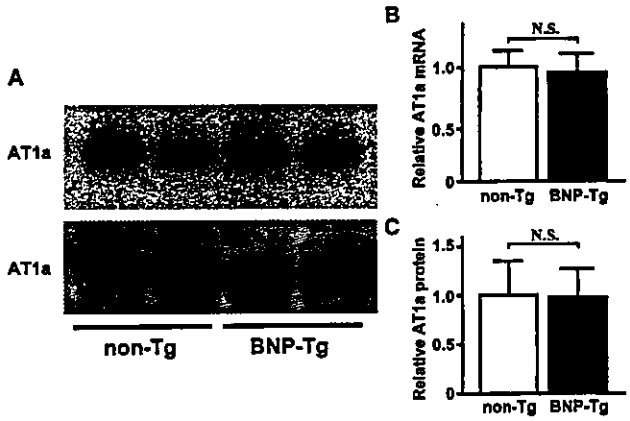

Fig. 1. *Expression of Ang II type 1a receptor (AT1a) mRNA and protein in the ventricles of unstimulated 10-week-old BNP-Tg and non-Tg mice. A: Representative Northern (top) and Western (bottom) blots of AT1a. B and C: Relative levels of AT1a mRNA (B) and protein (C) determined from the respective blots by densitometry. Values are the means±SEM (n=10); N.S., not significant.*

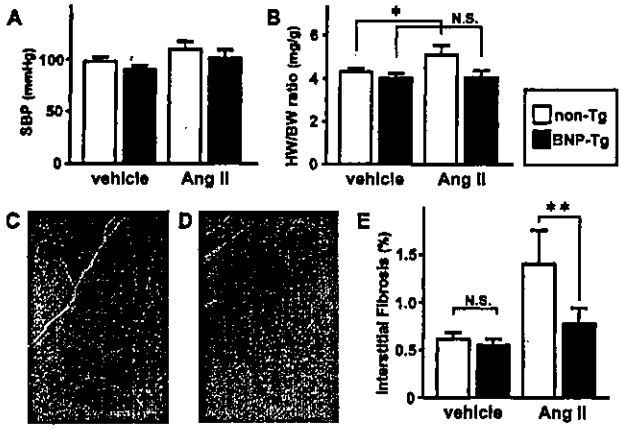

Fig. 2. *Effects of chronic Ang II infusion on SBP, HW/BW, and interstitial fibrosis. A: SBP measured by the tail-cuff method in conscious BNP-Tg and non-Tg mice infused with Ang II (0.6 mg/kg/day) or vehicle for 1 week. B: Ratios of heart weight (mg) to body weight (g) (HW/BW) in BNP-Tg and non-Tg mice infused with Ang II (0.6 mg/kg/day) or vehicle for 2 weeks. C and D: Representative micrographs showing van Gieson staining of the left ventricle from a non-Tg (C) and a BNP-Tg mouse (D). Red staining is characteristic of collagen matrix (interstitial fibrosis). E: Relative levels of interstitial fibrosis (%) determined as the ratios of the areas of van Gieson-stained interstitial fibrosis to the total left ventricular area. Perivascular fibrosis is not included. Values are the means±SEM (n=8); * p<0.01 vs. vehicle group, ** p<0.001 vs. non-Tg mice, N.S., not significant.*

formed as previously described (*15*). A murine AT1a probe was prepared as previously reported (*16*), and a human c-*fos* genomic probe was purchased from Takara Shuzo Co. (Kyoto, Japan).

Statistical Analysis

Data are expressed as the mean±SEM. Analysis of variance (ANOVA) with post hoc Fisher's tests was used to evaluate differences. Values of $p<0.05$ were considered to indicate statistical significance.

Results

Expression of Ventricular AT1a

Before analyzing the responses to Ang II, we compared the basal expression of AT1a in the ventricles of BNP-Tg and non-Tg mice and found no significant difference in the expression of AT1a mRNA (Fig. 1A and B) or protein (Fig. 1A and C).

Effects of Chronic Ang II Infusion on SBP, HW/BW, and Interstitial Fibrosis

SBP was about 5 mmHg lower in conscious BNP-Tg mice than non-Tg mice (92.6±1.0 *vs.* 97.7±0.8 mmHg, $p<0.01$), but chronic Ang II infusion (0.6 mg/kg/day) increased SBP to the same degree (by about 10 mmHg) in both groups (8.3±0.3 and 10.9±0.5 mmHg in BNP-Tg and non-Tg mice, respectively) (Fig. 2A). Among vehicle-treated mice, HW/BW ratios tended to be smaller in BNP-Tg than non-Tg mice, but the difference was not significant (4.04±0.21 *vs.* 4.32±0.07 mg/g, $p=0.26$); there was also no difference in the levels of left ventricular interstitial fibrosis (0.55±0.03 and 0.62±0.03% in BNP-Tg and non-Tg, respectively). Chronic Ang II infusion significantly increased HW/BW ratios (5.13±0.17 mg/g) (Fig. 2B) and interstitial fibrosis (1.41±0.09%) (Fig. 2C–E) in non-Tg mice, but had little effect in BNP-Tg mice (4.07±0.14 mg/g and 0.77±0.05% for HW/BW ratios and interstitial fibrosis, respectively).

Blood Pressure Elevation after Acute Ang II Injection

As shown in Fig. 3A, basal mean blood pressure (BP) measured under anesthesia from the carotid artery was 10–20 mmHg lower in BNP-Tg mice than in non-Tg mice (61.8±3.1 *vs.* 75.3±2.5 mmHg, $p<0.01$). In both groups, BP rapidly increased after acute injection of Ang II (0.3 mg/kg), peaking within about 5 min (after an about 60 mmHg increase), and then declined over a period of about 10 min. The change in mean BP (Δmean BP)—i.e., the difference between the peak and basal mean BPs—also did not significantly differ between the two groups (60.7±2.4 and 63.3±5.1 mmHg in BNP-Tg and non-Tg mice, respectively) (Fig. 3B), nor did the area under the BP curve (over basal BP level, until 15 min after Ang II injection) (1.91±0.16 and

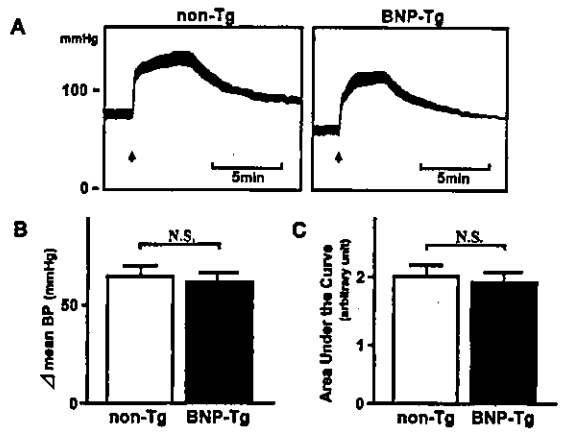

Fig. 3. *Changes in mean blood pressure (BP) evoked by acute injection of Ang II (0.3 mg/kg). A: Representative traces showing arterial BP in an anesthetized BNP-Tg (right) and non-Tg (left) mouse. The arrows indicate the beginning of the Ang II injection. B and C: Changes in mean BP (Δmean BP), measured as the difference between peak and basal mean BP (B), and the areas under the BP curve (over basal BP level, until 15 min after Ang II injection) (C). Values are the means±SEM* (n=*8*).

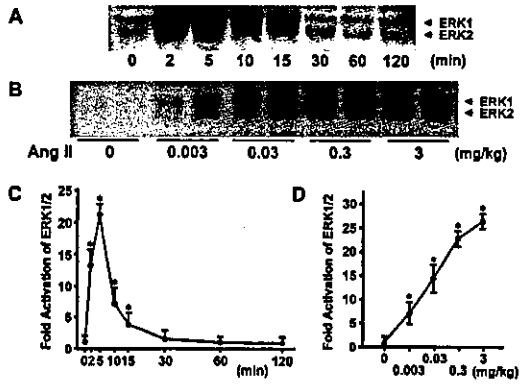

Fig. 4. *Time course and dose-dependency of Ang II-induced activation of ventricular ERK in non-Tg mice. Phosphorylation of ERK1/2 was examined by immunoblotting with an anti-phospho-ERK1/2 antibody. A: Representative Western blots of phospho-ERK1/2 in ventricles harvested at the indicated times after injection with Ang II (0.3 mg/kg). B: Representative Western blots of phospho-ERK1/2 in the ventricles harvested 5 min after injection with the indicated dose of Ang II. C and D: Time course (C) and dose-response (D) curves showing relative levels of ventricular ERK1/2 activity. Phospho-ERK1/2 was measured densitometrically from immunoblots like those in panels A and B and normalized to the control level (at 0 min), which was assigned a value of 1. Values are the means±SEM* (n=*5–10*); * $p<0.01$ vs. *control group.*

2.00±0.18 in BNP-Tg and non-Tg mice, respectively) (Fig. 3C).

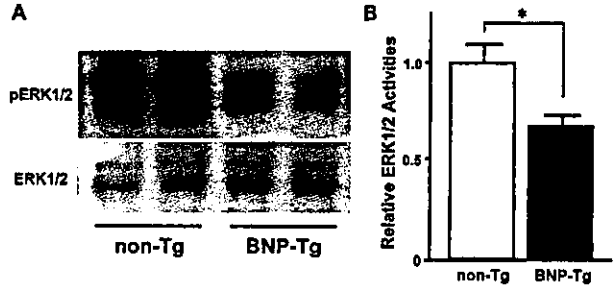

Fig. 5. *Comparison between left ventricular ERK activities in BNP-Tg and those in non-Tg mice. A: Representative Western blots showing phospho-ERK1/2 (pERK1/2, top) and ERK1/2 (bottom) in ventricles harvested 5 min after injection of Ang II (0.3 mg/kg). B: Phospho-ERK1/2 and ERK1/2 were measured densitometrically from immunoblots like those in panel A. The proportion of phospho-ERK1/2 in BNP-Tg mice was normalized to that in non-Tg mice, which was assigned a value of 1. Values are the means±SEM* (n=*10*); * $p<0.01$ vs. *non-Tg mice.*

Ventricular ERK Activation in Ang II-Injected Mice

Basal ERK activity did not differ between the ventricles of BNP-Tg and non-Tg mice, and chronic infusion of Ang II had little effect on ventricular ERK activity (data not shown). On the other hand, acute injection of Ang II (0.3 mg/kg) into non-Tg mice induced a significant increase in ERK1/2 activation, as indicated by the enzyme's phosphorylation. Levels of phospho-ERK1/2 increased rapidly, reaching a peak within 5 min, and then returned to baseline within 30 min (Fig. 4A and C). The effect of Ang II on ERK activation was dose-dependent, with a >25-fold increase at a dose of 3 mg/kg (Fig. 4B and D). Comparison with BNP-Tg mice showed that overexpression of BNP significantly (33%) diminished Ang II-induced ERK1/2 activation (Fig. 5).

Ventricular c-*fos* mRNA Expression

Acute injection of Ang II (0.3 mg/kg) into non-Tg mice induced significant increases in ventricular expression of c-*fos* mRNA that peaked within 30 min (Fig. 6A and B). Comparison with BNP-Tg mice showed that overexpression of BNP significantly (45%) diminished c-*fos* expression measured 30 min after Ang II injection (Fig. 6C and D).

Ventricular MKP Expression

To investigate the mechanism by which BNP inhibits the ERK–c-*fos* pathway *in vivo*, we assessed the expression of MKP-1 and -2 in the ventricles of BNP-Tg and non-Tg mice (Fig. 7). It is notable that the expression of both these enzymes was significantly (27% and 15%, respectively) induced in BNP-Tg mice (Fig. 7B and C).

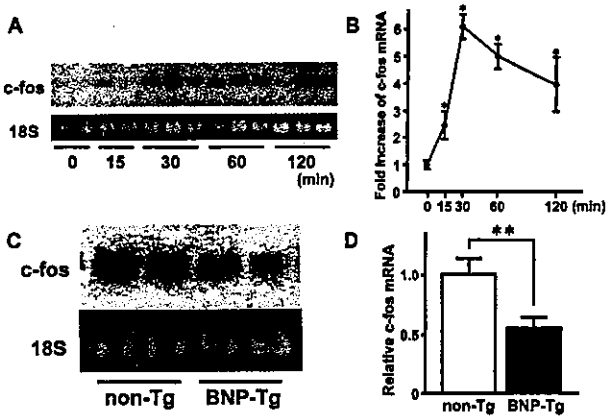

Fig. 6. *Ventricular expression of* c-fos *mRNA following acute injection of Ang II (0.3 mg/kg). A: Representative Northern blots showing the time course of* c-fos *mRNA expression. B:* c-fos *mRNA was measured densitometrically from immunoblots like those in panel A and normalized to the control level (at 0 min), which was assigned a value of 1. C: Representative Northern blots showing* c-fos *mRNA expression in ventricles from BNP-Tg and non-Tg mice harvested 30 min after acute injection of Ang II (0.3 mg/kg). D: Relative levels of ventricular* c-fos *mRNA expression normalized to 18S expression in BNP-Tg and non-Tg mice. Values of symbols (B) and bars (D) are the means±SEM* (n=5–8); * $p<0.01$ vs. *control;* ** $p<0.01$ vs. *non-Tg mice.*

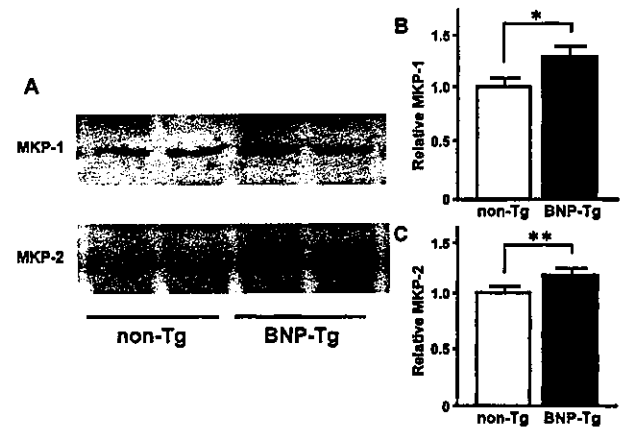

Fig. 7. *MKP-1 and -2 expression in the ventricles of unstimulated BNP-Tg and non-Tg mice. A: Representative Western blots of MKP-1 (top) and MKP-2 (bottom). B and C: Relative levels of MKP-1 (B) and MKP-2 (C) expression in BNP-Tg and non-Tg mice. MKPs were measured densitometrically from blots like those in panel A; levels in non-Tg mice were assigned a value of 1. Values are the means± SEM* (n=8); * $p<0.05$, ** $p<0.01$ vs. *non-Tg mice.*

Ventricular MEK Activation in Ang II-Injected BNP-Tg Mice

Finally, we examined the effects of Ang II on the ventricular levels of activated (phospho-) ERK kinase (MEK1/2), the MAPK kinase directly responsible for activation of ERK1/2. We found that in both BNP-Tg and non-Tg mice, acute injection of Ang II (0.3 mg/kg) increased the levels of phopho-MEK1/2 within 5 min (Fig. 8A), but that the effect was significantly (33%) diminished in BNP-Tg mice (Fig. 8B).

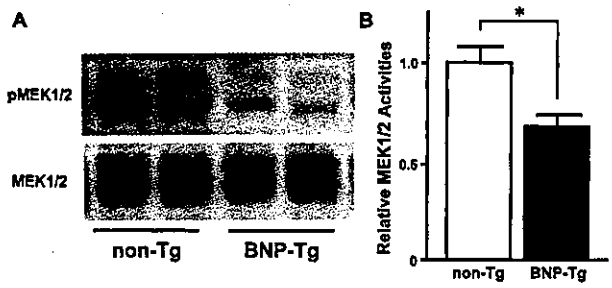

Fig. 8. *Comparison between ventricular MEK activities in BNP-Tg and those in non-Tg mice. A: Representative Western blots showing phospho-MEK1/2 (pMEK1/2, top) and MEK1/2 (bottom) in ventricles harvested 5 min after injection of Ang II (0.3 mg/kg). B: Phospho-MEK1/2 and MEK1/2 were measured densitometrically from immunoblots like those in panel A. The proportion of phospho-MEK1/2 in BNP-Tg mice was normalized to that in non-Tg mice, which was assigned a value of 1. Values are the means±SEM* (n=8); * $p<0.01$ vs. *non-Tg mice.*

Discussion

In the present study, we demonstrate that elevated circulating BNP inhibits the ventricular hypertrophy and fibrosis induced by Ang II in BNP-Tg mice. This finding suggests that NPs may not only improve the hemodynamics of CHF patients, but may also improve the long-term prognosis of CHF patients in the manner of ACE inhibitors through their cardioprotective effects.

Moreover, the data presented in this report show that elevated circulating BNP inhibits Ang II-induced activation of the ERK pathway. To our knowledge, this is the first report of crosstalk between NPs and the ERK pathway in the heart *in vivo*. A number of studies have demonstrated the key roles played by hypertrophic mediators in the ERK pathway (*17–21*). But while NPs and GC-A signaling are known to be involved in the regulation of cardiac hypertrophy and fibrosis (*8–10*), little was known about the *in vivo* mechanism by which NPs affect cardiac hypertrophy and fibrosis.

BNP-Tg mice exhibited reduced cardiac hypertrophy and fibrosis when chronically infused with Ang II. Although basal BP in BNP-Tg mice was lower than that in non-Tg mice, Ang II increased BP to the same degree in both groups; moreover, ventricular expression of AT1a was the same in BNP-Tg and non-Tg mice. This means that differences in extracellular stimuli—*i.e.*, humoral and mechanical factors—cannot account for the antihypertrophic and antifi-

brotic effects of BNP. What, then, is the mechanism of the antihypertrophic and antifibrotic actions of BNP?

The MAPK family members ERK, p38 MAPK, and c-Jun *N*-terminal kinases (JNKs) are known to be very important mediators of cardiac hypertrophy (*17–25*). In particular, the ERK pathway has been very frequently investigated due to its importance as a hypertrophic mediator. We therefore examined the effects of BNP on Ang II-induced activation of the ERK pathway and found that Ang II-induced ERK activation was significantly diminished in the ventricles of BNP-Tg mice, as was expression of c-*fos*, one of the immediate early response genes up-regulated in cardiac hypertrophy (*26–28*). In addition, because ANP was previously shown to induce expression of MKP-1 in glomerular mesangial cells, renal tubular cells, and endothelial cells (*29–31*), we assessed the ventricular expression of MKP-1 and -2 and found it to be significantly higher in BNP-Tg than in non-Tg mice. With regard to ventricular expression of MKP-1, Hiroi *et al.* reported that Ang II increases MKP-1 gene expression *via* negative feedback in cultured cardiac myocytes (*32*). But in our study, there was a difference in the expression of MKPs between BNP-Tg and non-Tg mice before Ang II infusion. This finding indicated that BNP increases ventricular MKP expression independent of any Ang II-related mechanism. MKPs dephosphorylate and thus inactivate ERK (*33*). In fact, in a previous study, Tg mice overexpressing MKP-1 showed no ERK activation and attenuated cardiac hypertrophy in response to aortic banding and catecholamine infusion (*21*). We therefore suggest that BNP-induced expression of MKPs in the ventricle reduces ERK activation at the same location, which in turn represses hypertrophy and fibrosis. It should be noted, however, that MKP-1 also inhibits activation of two other MAPKs, p38 MAPK and JNK (*21*), which might also have contributed to the antihypertrophic and antifibrotic effects of BNP.

Ang II-induced activation of MEK, the MAPK kinase directly responsible for activation of ERK, was also significantly repressed in mice overexpressing BNP. Suhasini *et al.* reported that in baby hamster kidney (BHK) cells, cGMP-dependent protein kinase inhibits the Ras-MAPK pathway by phosphorylating c-Raf kinase on Ser43, thereby inhibiting its activation (*34*). Because BNP increases the level of cGMP *via* GC-A, we suggest that BNP stimulates phosphorylation of c-Raf kinase, which would inhibit its activation and in turn inhibit activation of MEK. It thus appears that BNP exerts its cardioprotective effects largely by acting upstream of ERK, on both MKP and MEK.

We also recently reported that phosphorylation of ERK and immune-mediated renal injury are attenuated in the kidneys of experimental nephritic BNP-Tg mice, and NPs inhibit ERK phosphorylation induced by Ang II in cultured mesangial cells (*14*). Several lines of evidence have shown that Ang II contributes to the progression of renal injury in experimental glomerulonephritis (GN), as demonstrated by the alleviation of renal injury in GN associated with the inhibition of Ang II generation as well as the pharmacologic blockade or genetic disruption of AT1 (*35–37*). Taken together, these findings indicate that BNP inhibits the ERK phosphorylation induced by Ang II in the nephritic kidney, and consequently attenuates renal injury in GN. This mechanism of the renoprotective effect of BNP is compatible with the mechanism of the cardioprotective effect of BNP shown in the present study. It seems likely that MKPs are also up-regulated in the kidney of BNP-Tg mice.

In summary, we have shown that Ang II-induced ventricular hypertrophy and fibrosis are diminished in mice overexpressing BNP and that these cardioprotective effects are attributable to the inhibition of ventricular activation of the MEK-ERK transduction pathway. Based on these findings, it is hoped that the cardioprotective efficacy of BNP will be further examined in clinical studies.

Acknowledgements

We thank Dr. H. Rakugi for providing anti-AT1a antibody and K. Okamura for her excellent secretarial work.

References

1. Yoshimura M, Yasue H, Morita E, *et al*: Hemodynamic, renal, and hormonal responses to brain natriuretic peptide infusion in patients with congestive heart failure. *Circulation* 1991; **84**: 1581–1588.
2. Holmes SJ, Espiner EA, Richards AM, Yandle TG, Frampton C: Renal, endocrine, and hemodynamic effects of human brain natriuretic peptide in normal man. *J Clin Endocrinol Metab* 1993; **76**: 91–96.
3. Marcus LS, Hart D, Packer M, *et al*: Hemodynamic and renal excretory effects of human brain natriuretic peptide infusion in patients with congestive heart failure: a double-blind, placebo-controlled, randomized crossover trial. *Circulation* 1996; **94**: 3184–3189.
4. Abraham WT, Lowes BD, Ferguson DA, *et al*: Systemic hemodynamic, neurohormonal, and renal effects of a steady-state infusion of human brain natriuretic peptide in patients with hemodynamically decompensated heart failure. *J Card Fail* 1998; **4**: 37–44.
5. Mills RM, LeJemtel TH, Horton DP, *et al*: Sustained hemodynamic effects of an infusion of nesiritide (human b-type natriuretic peptide) in heart failure: a randomized, double-blind, placebo-controlled clinical trial: Natrecor Study Group. *J Am Coll Cardiol* 1999; **34**: 155–162.
6. Colucci WS, Elkayam U, Horton DP, *et al*: Intravenous nesiritide, a natriuretic peptide, in the treatment of decompensated congestive heart failure: Nesiritide Study Group. *N Engl J Med* 2000; **343**: 246–253.
7. Yusuf S, Lonn E, Bosch J, Gerstein H: Summary of randomized trials of angiotensin converting enzyme inhibitors. *Clin Exp Hypertens* 1999; **21**: 835–845.
8. John SW, Krege JH, Oliver PM, *et al*: Genetic decreases in atrial natriuretic peptide and salt-sensitive hypertension. *Science* 1995; **267**: 679–681.
9. Tamura N, Ogawa Y, Chusho H, *et al*: Cardiac fibrosis in

mice lacking brain natriuretic peptide. *Proc Natl Acad Sci USA* 2000; **97**: 4239–4244.
10. Lopez MJ, Wong SK, Kishimoto I, *et al*: Salt-resistant hypertension in mice lacking the guanylyl cyclase-A receptor for atrial natriuretic peptide. *Nature* 1995; **378**: 65–68.
11. Li Y, Kishimoto I, Saito Y, *et al*: Guanylyl cyclase-A inhibits angiotensin II type 1A receptor-mediated cardiac remodeling, an endogenous protective mechanism in the heart. *Circulation* 2002; **106**: 1722–1728.
12. Ogawa Y, Itoh H, Tamura N, *et al*: Molecular cloning of the complementary DNA and gene that encode mouse brain natriuretic peptide and generation of transgenic mice that overexpress the brain natriuretic peptide gene. *J Clin Invest* 1994; **93**: 1911–1921.
13. Suda M, Ogawa Y, Tanaka K, *et al*: Skeletal overgrowth in transgenic mice that overexpress brain natriuretic peptide. *Proc Natl Acad Sci USA* 1998; **95**: 2337–2342.
14. Suganami T, Mukoyama M, Sugawara A, *et al*: Overexpression of brain natriuretic peptide in mice ameliorates immune-mediated renal injury. *J Am Soc Nephrol* 2001; **12**: 2652–2663.
15. Nakagawa O, Ogawa Y, Itoh H, *et al*: Rapid transcriptional activation and early mRNA turnover of brain natriuretic peptide in cardiocyte hypertrophy: evidence for brain natriuretic peptide as an "emergency" cardiac hormone against ventricular overload. *J Clin Invest* 1995; **96**: 1280–1287.
16. Burson JM, Aguilera G, Gross KW, Sigmund CD: Differential expression of angiotensin receptor 1A and 1B in mouse. *Am J Physiol* 1994; **267**: E260–E267.
17. Yamazaki T, Komuro I, Kudoh S, *et al*: Endothelin-1 is involved in mechanical stress-induced cardiomyocyte hypertrophy. *J Biol Chem* 1996; **271**: 3221–3228.
18. Bogoyevitch MA, Andersson MB, Gillespie-Brown J, *et al*: Adrenergic receptor stimulation of the mitogen-activated protein kinase cascade and cardiac hypertrophy. *Biochem J* 1996; **314**: 115–121.
19. Olson EN, Molkentin JD: Prevention of cardiac hypertrophy by calcineurin inhibition: hope or hype? *Circ Res* 1999; **84**: 623–632.
20. Hunter JJ, Tanaka N, Rockman HA, Ross J Jr, Chien KR: Ventricular expression of a MLC-2v-ras fusion gene induces cardiac hypertrophy and selective diastolic dysfunction in transgenic mice. *J Biol Chem* 1995; **270**: 23173–23178.
21. Bueno OF, De Windt LJ, Lim HW, *et al*: The dual-specificity phosphatase MKP-1 limits the cardiac hypertrophic response *in vitro* and *in vivo*. *Circ Res* 2001; **88**: 88–96.
22. Zechner D, Thuerauf DJ, Hanford DS, McDonough PM, Glembotski CC: A role for the p38 mitogen-activated protein kinase pathway in myocardial cell growth, sarcomeric organization, and cardiac-specific gene expression. *J Cell Biol* 1997; **139**: 115–127.
23. Wang Y, Huang S, Sah VP, *et al*: Cardiac muscle cell hypertrophy and apoptosis induced by distinct members of the p38 mitogen-activated protein kinase family. *J Biol Chem* 1998; **273**: 2161–2168.
24. Kudoh S, Komuro I, Mizuno T, *et al*: Angiotensin II stimulates c-Jun NH_2-terminal kinase in cultured cardiac myocytes of neonatal rats. *Circ Res* 1997; **80**: 139–146.
25. Ramirez MT, Sah VP, Zhao XL, Hunter JJ, Chien KR, Brown JH: The MEKK-JNK pathway is stimulated by alpha 1-adrenergic receptor and ras activation and is associated with *in vitro* and *in vivo* cardiac hypertrophy. *J Biol Chem* 1997; **272**: 14057–14061.
26. Izumo S, Nadal-Ginard B, Mahdavi V: Protooncogene induction and reprogramming of cardiac gene expression produced by pressure overload. *Proc Natl Acad Sci USA* 1988; **85**: 339–343.
27. Sadoshima J, Jahn L, Takahashi T, Kulik TJ, Izumo S: Molecular characterization of the stretch-induced adaptation of cultured cardiac cells: an *in vitro* model of load-induced cardiac hypertrophy. *J Biol Chem* 1992; **267**: 10551–10560.
28. Babu GJ, Lalli MJ, Sussman MA, Sadoshima J, Periasamy M: Phosphorylation of elk-1 by MEK/ERK pathway is necessary for c-fos gene activation during cardiac myocyte hypertrophy. *J Mol Cell Cardiol* 2000; **32**: 1447–1457.
29. Sugimoto T, Haneda M, Togawa M, *et al*: Atrial natriuretic peptide induces the expression of MKP-1, a mitogen-activated protein kinase phosphatase, in glomerular mesangial cells. *J Biol Chem* 1996; **271**: 544–547.
30. Hannken T, Schroeder R, Stahl RA, Wolf G: Atrial natriuretic peptide attenuates ANG II-induced hypertrophy of renal tubular cells. *Am J Physiol Renal Physiol* 2001; **281**: F81–F90.
31. Kiemer AK, Weber NC, Furst R, Bildner N, Kulhanek-Heinze S, Vollmar AM: Inhibition of p38 MAPK activation *via* induction of MKP-1: atrial natriuretic peptide reduces TNF-alpha-induced actin polymerization and endothelial permeability. *Circ Res* 2002; **90**: 874–881.
32. Hiroi Y, Hiroi J, Kudoh S, Yazaki Y, Nagai R, Komuro I: Two distinct mechanisms of angiotensin II-induced negative regulation of the mitogen-activated protein kinases in cultured cardiac myocytes. *Hypertens Res* 2001; **24**: 385–394.
33. Haneda M, Sugimoto T, Kikkawa R: Mitogen-activated protein kinase phosphatase: a negative regulator of the mitogen-activated protein kinase cascade. *Eur J Pharmacol* 1999; **365**: 1–7.
34. Suhasini M, Li H, Lohmann SM, Boss GR, Pilz RB: Cyclic-GMP-dependent protein kinase inhibits the Ras/mitogen-activated protein kinase pathway. *Mol Cell Biol* 1998; **18**: 6983–6994.
35. Hisada Y, Sugaya T, Yamanouchi M, *et al*: Angiotensin II plays a pathogenic role in immune-mediated renal injury in mice. *J Clin Invest* 1999; **103**: 627–635.
36. Ruiz-Ortega M, Gonzalez S, Seron D, *et al*: ACE inhibition reduces proteinuria, glomerular lesions and extracellular matrix production in a normotensive rat model of immune complex nephritis. *Kidney Int* 1995; **48**: 1778–1791.
37. Yayama K, Makino J, Takano M, Okamoto H: Role of angiotensin II in the transforming growth factor-β1 expression of rat kidney in anti-glomerular basement membrane antiserum-induced glomerulonephritis. *Biol Pharm Bull* 1995; **18**: 687–690.

Different Differentiation Kinetics of Vascular Progenitor Cells in Primate and Mouse Embryonic Stem Cells

Masakatsu Sone, MD; Hiroshi Itoh, MD, PhD; Jun Yamashita, MD, PhD; Takami Yurugi-Kobayashi, MD; Yutaka Suzuki, PhD; Yasushi Kondo, PhD; Akane Nonoguchi; Naoki Sawada, MD, PhD; Kenichi Yamahara, MD; Kazutoshi Miyashita, MD; Kwijun Park, MD; Masabumi Shibuya, MD, PhD; Shinji Nito, PhD; Shin-Ichi Nishikawa, MD, PhD; Kazuwa Nakao, MD, PhD

Background—We demonstrated that vascular endothelial growth factor receptor 2 (VEGF-R2)-positive cells derived from mouse embryonic stem (ES) cells can differentiate into both endothelial cells and mural cells to suffice as vascular progenitor cells (VPCs). Here we examined whether VPCs occur in primate ES cells and investigated the differences in VPC differentiation kinetics between primate and mouse ES cells.

Methods and Results—In contrast to mouse ES cells, undifferentiated monkey ES cells expressed VEGF-R2. By culturing these undifferentiated ES cells for 4 days on OP9 feeder layer, VEGF-R2 expression disappeared, and then reappeared after 8 days of differentiation. We then isolated these VEGF-R2–positive and vascular endothelial cadherin (VEcadherin)-negative cells by flow cytometry sorting. Additional 5-day reculture of these VEGF-R2$^+$ VEcadherin$^-$ cells on OP9 feeder layer resulted in the appearance of platelet endothelial cell adhesion molecule-1 (PECAM1)-positive, VEcadherin-positive, endothelial nitric oxide synthase (eNOS)-positive endothelial cells. On a collagen IV-coated dish in the presence of serum, these cells differentiated into smooth muscle actin (SMA)-positive and calponin-positive mural cells (pericytes or vascular smooth muscle cells). Addition of 50ng/mL VEGF to the culture on a collagen IV-coated dish resulted in the appearance of PECAM1$^+$ cells surrounded by SMA$^+$ cells. In addition, these differentiated VEGF-R2$^+$ cells can form tube-like structures in a 3-dimensional culture.

Conclusion—Our findings indicate that differentiation kinetics of VPCs derived from primate and mouse ES cells were different. Differentiated VEGF-R2$^+$ VEcadherin$^-$ cells can act as VPCs in primates. To seek the clinical potential of VPCs for vascular regeneration, investigations of primate ES cells are indispensable. (***Circulation.*** **2003;107:2085-2088.)**

Key Words: angiogenesis ■ cells ■ endothelium ■ muscle, smooth ■ vessels

Embryonic stem (ES) cells with pluripotency and self-renewal are now highlighted as promising cell sources for regeneration medicine. Previously we demonstrated that mouse ES cell-derived vascular endothelial growth factor receptor-2 (VEGF-R2)-positive cells can differentiate into both endothelial cells and mural cells (pericytes and vascular smooth muscle cells) and reproduce the vascular organization process.[1] Vascular cells derived from VEGF-R2$^+$ cells can organize vessel-like structures in a 3-dimensional culture. Mouse ES cell-derived VEGF-R2$^+$ cells can, thus, serve as vascular progenitor cells (VPCs). Furthermore, we have reported that implantation of mouse ES-derived vascular cells into nude mice significantly augmented blood flow in an adult neoangiogenesis model, which suggests the usefulness of ES cell-derived VPCs for vascular regeneration medicine.[2]

Recently primate embryonic stem cell lines were established from blastocysts of both humans and monkeys.[3–6] Primate ES cells possess a number of characteristics distinct from mouse ES cells, such as surface antigens, leukemia inhibitory factor (LIF)-independence, and long doubling times.[3–7] Recent study showed that VEGF-R2 was expressed in undifferentiated human ES cells, unlike in mouse ES cells,[8,9] and continuously expressed during differentiation in embryoid body (EB) formation. It has also been demonstrated that platelet endothelial cell adhesion molecule-1 (PECAM1)-positive cells can be isolated from human EBs,

Received December 31, 2002; revision received March 12, 2003; accepted March 13, 2003.

From the Department of Medicine and Clinical Science (M.S., H.I., T.Y.-K., A.N., N.S., K.Y., K.M., K.P., K.N.) and the Department of Molecular Genetics (J.Y., S.-I.N.), Kyoto University Graduate School of Medicine, Kyoto; the Discovery Research Laboratory, Tanabe Seiyaku Co, Ltd, Osaka (Y.S., Y.K., S.N.); the Department of Genetics, Institute of Medical Science, University of Tokyo, Tokyo (M.S.); and the Center for Developmental Biology, RIKEN, Kobe (S.-I.N.), Japan.

Correspondence to Hiroshi Itoh, MD, PhD, Department of Medicine and Clinical Science, Kyoto University Graduate School of Medicine, 54 Shogoin Kawahara-cho, Sakyo-ku, Kyoto 606-8507 Japan. E-mail hiito@kuhp.kyoto-u.ac.jp

Circulation is available at http://www.circulationaha.org

DOI: 10.1161/01.CIR.0000070022.78747.1B

and they can act as endothelial cells.[9] However, the vascular differentiation process of primate cells has not been demonstrated, and VPCs that can differentiate into both endothelial cells and mural cells have not been characterized in the primates. To elucidate the vascular differentiation process of primate cells and to seek the clinical potential of VPCs for vascular regeneration therapy with the use of an in vitro 2-dimensional differentiation system of ES cells that we established,[10,11] we examined whether and how VPCs occur in primate ES cells in comparison to mouse ES cells.

Methods

Cell Culture

Cynomolgus monkey ES cell lines were established, and their pluripotency was confirmed by teratoma formation in severe combined immunodeficiency mice, as described previously.[6,12] Undifferentiated ES cells were maintained as described.[6,12] OP9 feeder cell lines that were established from mouse calvaria were maintained as described previously.[11,13,14]

To induce differentiation, undifferentiated ES cells were cultured on OP9 feeder layer in differentiation medium (minimal essential medium [GIBCO] supplemented with 10% fetal calf serum (FCS) and 5×10^{-5} M2-mercaptoethanol).[11] Sorted VEGF-R2$^+$ cells were re-cultured on an OP9 feeder layer or collagen IV-coated dish with differentiation medium. Three-dimensional culture was performed as described.[1]

Flow Cytometry and Cell Sorting

At different time points during the differentiation process, cultured cells were harvested by cell dissociation buffer (GIBCO). Flow cytometry analysis and cell sorting were as discribed.[10,11] Monoclonal antibody for VEGF-R2, which we developed,[15] was labeled with Alexa-647 in our laboratory (monoclonal antibody labeling kit, molecular probes). PE-conjugated vascular endothelial cadherin (VEcadherin) antibody and fluorescein isothiocyanate-conjugated PECAM1 antibody were purchased from BD Biosciences. To test the differentiation potential of VEGF-R2$^+$ cells, sorted cells were plated into a collagen IV-coated 96-well dish at the density of 2.5×10^3 cells per well, or plated on OP9 feeder layer in a 24-well dish at 1×10^4 cells per well.

Immunohistochemistry

Staining of culture cells on dishes was as described.[1,11] Monoclonal antibody for smooth muscle actin (SMA) was purchased from Sigma, those for calponin and smooth muscle myosin heavy chain (SMMHC) were purchased from DAKO, and those for PECAM1, VEcadherin, and endothelial nitric oxide synthase (eNOS) were purchased from BD Biosciences.

Results

Although undifferentiated mouse ES cells did not express VEGF-R2, most of undifferentiated monkey ES cells were positive for VEGF-R2 (data not shown). Mouse ES cells differentiated into VEGF-R2$^+$ cells during a 4-day differentiation on OP9 feeder layer. These mouse VEGF-R2$^+$ cells differentiated into endothelial cells during 4 days of re-culturing on a collagen IV-coated dish or OP9 feeder layer.[1,11] In contrast, however, we could not induce endothelial cells from VEGF-R2$^+$ undifferentiated monkey ES cells in the same condition (data not shown). Thus, we examined VEGF-R2 expression on monkey ES cells during differentiation.

Undifferentiated monkey ES cells were dissociated to single cells and plated on an OP9 feeder layer to induce differentiation (Figure 1A). As shown in Figure 1B, VEGF-R2 was expressed in undifferentiated monkey ES cells (day 0), but disappeared during a 4-day differentiation on OP9 feeder layer, and then reappeared after 8 days of differentiation. VEcadherin$^+$ cells appeared at day 10 of differentiation. Alkaline phosphatase activity, which was reported to be detected in undifferentiated ES cells[3,5] but not in mature vascular cells, was clearly detected in undifferentiated ES cells but not in the cells that were cultured for 8 days on an OP9 feeder layer (Figure 1C and 1D), indicating that VEGF-R2$^+$ cells at 8-day differentiation are apparently distinct from those observed in undifferentiated ES cells.

VEGF-R2$^+$ VEcadherin$^-$ cells were purified by flow cytometry sorting at day 8 (Figure 1A). Additional 5-day culturing of VEGF-R2$^+$ VEcadherin$^-$ cells on an OP9 feeder layer resulted in the appearance of PECAM1$^+$ cells (Figure 2A), which were also positive for VEcadherin and eNOS (Figure 2B and 2C). On the other hand, on a collagen IV-coated dish with 10% FCS, more than 90% of VEGF-R2$^+$ VEcadherin$^-$ cells became positive for SMA (Figure 2D) and calponin (Figure 2E) after an additional 5 days of culturing. Some were positive for SMMHC (Figure 2F). In this culturing condition, PECAM1$^+$ endothelial cells did not appear. In contrast, addition of 50ng/mL VEGF to culture on a collagen IV-coated dish resulted in the appearance of PECAM1$^+$ cells (about 20% of total cells) that were surrounded by SMA$^+$ cells (Figure 2G). VEGF-R2$^+$ VEcadherin$^-$ cells at day 10 also could differentiate into endothelial cells and mural cells similarly to day 8. VEGF-R2$^+$ VEcadherin$^-$ cells doubled themselves in about 44 hours on a collagen IV-coated dish with VEGF and FCS. Almost all of the VEGF-R2$^+$ VEcadherin$^+$ cells obtained by flow cytometry sorting at day 10 became positive for PECAM1 after an additional 5 days of culturing on a collagen IV-coated dish with 10% FCS.

We further examined whether VEGF-R2$^+$ cells can form vascular structure in vitro. Aggregates of several hundred VEGF-R2$^+$ cells were cultivated in collagen I-A gels with 10% FCS, 50ng/mL VEGF, 50ng/mL basic fibroblast growth factor, and 100 pM phorbol myristate acetate. The cells migrated out from the aggregates and formed cord-like structures within 3 days (Figure 2H).

Discussion

In the previous study,[1] we showed that VEGF-R2$^+$ cells in 4-day differentiation of mouse ES cells can differentiate into 2 major vascular cell types (endothelial cells and mural cells) in vitro and in vivo. Unlike mouse ES cells, undifferentiated monkey ES cells were already expressing VEGF-R2, similar to human ES cells. VEGF-R2 expression on monkey ES cells disappeared during 4-day differentiation on an OP9 feeder layer, and then re-expressed after 8 days of differentiation (Figure 1C). VEGF-R2–expressing cells on day 8 were different from VEGF-R2$^+$ undifferentiated monkey ES cells. First, the former did not show alkaline phosphatase activity as the latter did. Second, the former could differentiate into endothelial cells but the latter could not. Thus, the VEGF-R2$^+$ cells that re-appeared at 8 days of differentiation in monkey ES cell differentiation seem to possess similar differentiation potentials to those in 4-day differentiation of mouse ES cells,

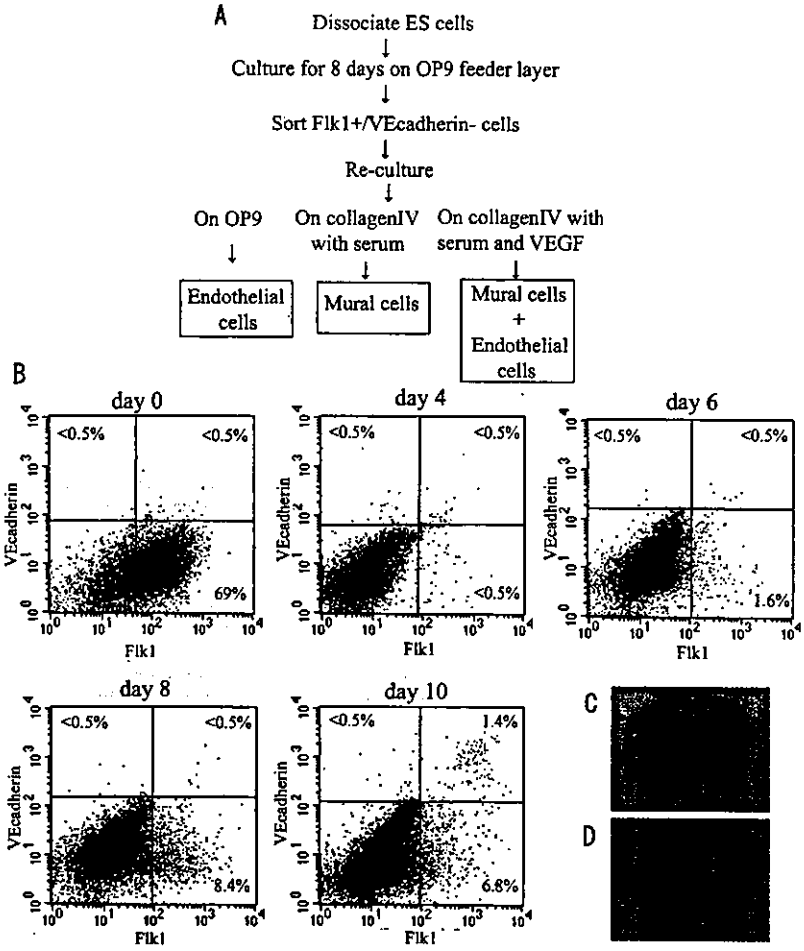

Figure 1. A, Schematic representation of the differentiation from ES cells to endothelial cells and mural cells. B, Flow cytometric analysis of the time course of differentiation of primate ES cells on an OP9 feeder layer. C, Alkaline phosphatase activity of undifferentiated ES cells on mouse embryonic fibroblast layer. D, Alkaline phosphatase activity of ES cells differentiated for 8 days on an OP9 feeder layer. Flk1 is a VEGF-R2. Scale bars: 100 μM.

whereas VEGF-R2 expression in undifferentiated monkey ES cells should be of less functional significance in vascular differentiation.

In the present study, we demonstrated that VEGF-R2$^+$ VEcadherin$^-$ cells that appeared at 8-days' differentiation in monkey ES cells give rise to both endothelial cells and mural cells and form vascular-like structures in a 3-dimentional culture in vitro. Our findings indicate that differentiated VEGF-R2$^+$ cells can act as VPCs in primates, and the differentiation kinetics of VPCs in primate and mouse ES cells were different. Thus, to seek the clinical potential of VPCs for vascular regeneration and to

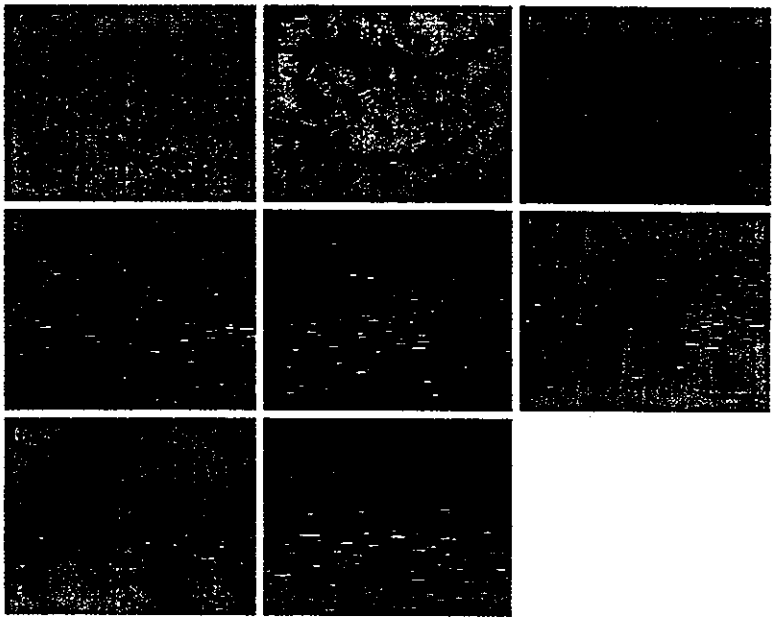

Figure 2. Immunohistochemical analysis of differentiation of primate ES cells into vascular cells (A through G). A through C, Immunostaining for endothelial cell markers: PECAM1 (A), VEcadherin (B), and eNOS (C). D through F, Immunostaining for mural cell markers: smooth muscle actin (D), calponin (E), and smooth muscle myosin heavy chain (F). G, Double immunostaining for PECAM1 (brown) and smooth muscle actin (blue). H, Tube formation of VEGF-R2$^+$ cell aggregates in 3-dimensional culture. Scale bars: B through G, 50 μM; A and H, 100 μM.

obtain novel insights in primate vascular development, investigations of primate ES cells are indispensable. Our novel in vitro vascular differentiation system using VPCs derived from primate ES cells is promising for dissecting the molecular and cellular mechanisms in the primate vascular development, to which the knock-out animal research approach is not available.

References

1. Yamashita J, Itoh H, Hirashima M, et al. Flk1-positive cells derived from embryonic stem cells serve as vascular progenitors. *Nature*. 2000;408: 92–96.
2. Yurugi-Kobayashi T, Itoh H, Yamashita J, et al. Effective contribution of transplanted vascular progenitor cells derived from embryonic stem cells to adult neovascularization in proper differentiation stage. *Blood*. 2003; 101:2675–2678.
3. Thomson JA, Kalishman J, Golos TG, et al. Isolation of a primate embryonic stem cell line. *Proc Natl Acad Sci U S A*. 1995;92:7844–7848.
4. Thomson JA, Itskovitz-Eldor J, Shapiro SS, et al. Embryonic stem cell lines derived from human blastocysts. *Science*. 1998;282:1145–1147.
5. Reubinoff BE, Pera MF, Fong CY, et al. Embryonic stem cell lines from human blastocysts: somatic differentiation in vitro. *Nat Biotechnol*. 2000; 18:399–404.
6. Suemori H, Tada T, Torii R, et al. Establishment of embryonic stem cell lines from cynomolgus monkey blastocysts produced by IVF or ICSI. *Dev Dyn*. 2001;222:273–279.
7. Amit M, Carpenter MK, Inokuma MS, et al. Clonally derived human embryonic stem cell lines maintain pluripotency and proliferative potential for prolonged periods of culture. *Dev Biol*. 2000;227:271–278.
8. Kaufman DS, Hanson ET, Lewis RL, et al. Hematopoietic colony-forming cells derived from human embryonic stem cells. *Proc Natl Acad Sci U S A*. 2001;98:10716–10721.
9. Levenberg S, Golub JS, Amit M, et al. Endothelial cells derived from human embryonic stem cells. *Proc Natl Acad Sci U S A*. 2002;99: 4391–4396.
10. Nishikawa SI, Nishikawa S, Hirashima M, et al. Progressive lineage analysis by cell sorting and culture identifies FLK1+VE-cadherin+ cells at a diverging point of endothelial and hemopoietic lineages. *Development*. 1998;125:1747–1757.
11. Hirashima M, Kataoka H, Nishikawa S, et al. Maturation of embryonic stem cells into endothelial cells in an in vitro model of vasculogenesis. *Blood*. 1999;93:1253–1263.
12. Kawasaki H, Suemori H, Mizuseki K, et al. Generation of dopaminergic neurons and pigmented epithelia from primate ES cells by stromal cell-derived inducing activity. *Proc Natl Acad Sci U S A*. 2002;99: 1580–1585.
13. Kodama H, Nose M, Niida S, et al. Involvement of the c-kit receptor in the adhesion of hematopoietic stem cells to stromal cells. *Exp Hematol*. 1994;22:979–984.
14. Kodama H, Nose M, Yamaguchi Y, et al. In vitro proliferation of primitive hemopoietic stem cells supported by stromal cells: evidence for the presence of a mechanism(s) other than that involving c-kit receptor and its ligand. *J Exp Med*. 1992;176:351–361.
15. Sawano A, Iwai S, Sakurai Y, et al. Flt-1, vascular endothelial growth factor receptor 1, is a novel cell surface marker for the lineage of monocyte-macrophages in humans. *Blood*. 2001;97:785–791.

Brief report

Effective contribution of transplanted vascular progenitor cells derived from embryonic stem cells to adult neovascularization in proper differentiation stage

Takami Yurugi-Kobayashi, Hiroshi Itoh, Jun Yamashita, Kenichi Yamahara, Hideyo Hirai, Takuya Kobayashi, Minetaro Ogawa, Satomi Nishikawa, Shin-Ichi Nishikawa, and Kazuwa Nakao

We demonstrated that Flk-1$^+$ cells derived from mouse embryonic stem (ES) cells can differentiate into both endothelial cells (ECs) and mural cells (MCs) to suffice as vascular progenitor cells (VPCs). In the present study, we investigated the importance of the stage of ES cell differentiation on effective participation in adult neovascularization. We obtained Flk-1$^+$ LacZ-expressing undifferentiated VPCs. Additional culture of these VPCs with vascular endothelial growth factor (VEGF) resulted in a mixture of ECs and MCs (differentiated VPCs). We injected VPCs subcutaneously into tumor-bearing mice. Five days after the injection, whereas undifferentiated VPCs were often detected as nonvascular cells, differentiated VPCs were more specifically incorporated into developing vasculature mainly as ECs. VPC-derived MCs were also detected in vascular walls. Furthermore, transplantation of differentiated VPCs augmented tumor blood flow in nude mice. These results indicate that a specific vascular contribution in adult neovascularization can be achieved by selective transplantation of ES cell–derived VPCs in appropriate differentiation stages, which should be the basis for vascular regeneration schemes. (Blood. 2003;101:2675-2678)

Introduction

Embryonic stem (ES) cells with totipotency and self-renewal are now highlighted as promising sources for regeneration medicine. Recently we demonstrated that ES cell-derived Flk-1$^+$ cells can differentiate into both endothelial cells (ECs) and mural cells (MCs; pericytes and vascular smooth muscle cells) and reproduce the vascular organization process.[1] Vascular endothelial growth factor (VEGF) promotes EC differentiation from vascular progenitor cells (VPCs). Vascular cells derived from Flk-1$^+$ cells can organize vessel-like structures in 3-dimensional culture. ES cell-derived Flk-1$^+$ cells can thus serve as VPCs.

To date, substantial trials on vascular regeneration using endothelial precursor/progenitor cells derived from somatic cells have been reported.[2-4] However, precise characterization of the transplanted cells or comparison of the effectiveness of cell differentiation stages to generate blood vessels has been scarce. We have established an in vitro vascular differentiation system using VPCs that can obtain ES cell–derived vascular cells at different stages of differentiation with homogeneity and in large quantities. Thus, in the present study, we examined the impact of differentiation stage differences of donor Flk-1$^+$ ES cells in transplantation on adult neoangiogenesis, to explore the potential of Flk-1$^+$ VPCs for vascular generation therapy.

Study design

Cell culture and sorting

Maintenance of CCE[5] ES cells (gift from M. J. Evans, Cambridge, United Kingdom) was as described previously.[6] To induce Flk-1$^+$ cells, ES cells were cultured on type IV collagen–coated dishes as reported previously.[6] Flk-1$^+$ VE-cadherin$^-$E-cadherin$^-$ cells were sorted by fluorescence-activated cell sorting (FACSVantage; Becton Dickinson, Bedford, MA) as described.[6,7] After 3 days of incubation on type IV collagen-coated dishes with 50 ng/mL VEGF (human $VEGF_{165}$; R & D Systems, Minneapolis, MN) in 10% fetal calf serum (FCS), cultured cells were harvested and further resorted by FACS. For serum-free culture, Flk-1$^+$ cells were incubated in SFO3 (Sanko Junyaku, Chiba, Japan) with 10 ng/mL platelet-derived growth factor-BB (PDGF-BB; Gibco BRL, Grand Island, NY) as described.[1] For detection of circulating LacZ$^+$ cells in peripheral blood by flow cytometry, we used FluoReporter LacZ flow cytometry kits (Molecular Probes, Eugene, OR).

Tumor transplantation and ES cell injection

Six- to 8-week-old nude (nu/nu) mice (SLC, Shizuoka, Japan) underwent subcutaneous transplantation of 1×10^6 C6 rat glioblastoma cells, which secrete large amounts of VEGF, in 0.1 mL phosphate-buffered saline (PBS) on right and left flanks as reported previously.[8] ES cells expressing *LacZ* gene (CCE/nLacZ) were generated as previously reported.[1] Seven days after tumor transplantation, C6 cells produced small tumors in both sides of the flank. We injected ES cell–derived VPCs in 0.1 mL PBS subcutaneously at 5 sites around the left tumor. Control (PBS only, right) and VPC-transplanted (left) tumors were excised 5 days after injection and sectioned into 50 blocks for whole-mount LacZ staining.

LDPI analysis of the tumor blood flow

We measured the ratios of VPCs transplanted (left) to control (right) tumor blood flow using a laser Doppler perfusion image (LDPI) analyzer (Moor Instruments, Devon, United Kingdom) 5 days after VPC transplantation.

From the Department of Medicine and Clinical Science, Department of Molecular Genetics, Kyoto University Graduate School of Medicine, Department of Microbiology, Kyoto Prefectural University of Medicine, Department of Pharmacology, Kyoto University Graduate School of Medicine, Kyoto, Japan; and Department of Cell Differentiation, Institute of Molecular Embryology and Genetics, Kumamoto University, Kumamoto, Japan.

Submitted June 26, 2002; accepted November 22, 2002. Prepublished online as *Blood* First Edition Paper, December 12, 2002; DOI 10.1182/blood-2002-06-1877.

Reprints: Hiroshi Itoh, Department of Medicine and Clinical Science, Kyoto University Graduate School of Medicine, 54 Shogoin Kawahara-cho, Sakyo-ku, Kyoto 606-8507 Japan; e-mail: hiito@kuhp.kyoto-u.ac.jp.

The publication costs of this article were defrayed in part by page charge payment. Therefore, and solely to indicate this fact, this article is hereby marked "advertisement" in accordance with 18 U.S.C. section 1734.

Results and discussion

Characterization of implanted ES cell–derived VPCs

Sorted Flk-1$^+$E-cadherin$^-$ cells did not express other EC (VE-cadherin, platelet-endothelial cell adhesion molecule 1 [PECAM-1], or CD34; Figure 1A-C) or MC (smooth muscle actin [SMA] or platelet-derived growth factor β [PDGF-β] receptor) markers (data not shown). We termed these cells "undifferentiated VPCs." After an additional 3 days of culture with 10% FCS and 50 ng/mL $VEGF_{165}$, Flk-1$^+$ cells differentiated into mixtures of ECs and MCs. The cells that retained Flk-1 expression (about 30%) became also positive for VE-cadherin, PECAM-1, and CD34, indicating the differentiation into ECs (Figure 1D-E). The cells that lost Flk-1 expression (about 70%) were negative for EC markers, but positive for SMA (Figure 1F-G) and other markers of differentiated vascular smooth muscle cells (smooth muscle myosin heavy chain, calponin, and SM22α; data not shown). These cell mixtures were designated "differentiated VPCs." We also sorted out a VE-cadherin$^+$ fraction of differentiated VPCs by FACS. Three-day treatment of undifferentiated VPCs with PDGF-BB resulted in selective induction of SMA$^+$ MCs, which were negative for Flk-1, VE-cadherin, and PECAM-1 (data not shown) in serum-free conditions (PDGF-BB–treated VPCs). Undifferentiated VPCs, differentiated VPCs (1×10^6 cells), VE-cadherin$^+$ fraction of differentiated VPCs (0.3×10^6 cells), or PDGF-BB–treated VPCs (0.7×10^6 cells) were implanted (Figure 1H-I) into nude mice. We also injected 0.5 to 1.0×10^6 undifferentiated and differentiated VPCs in PBS into the tail vein.

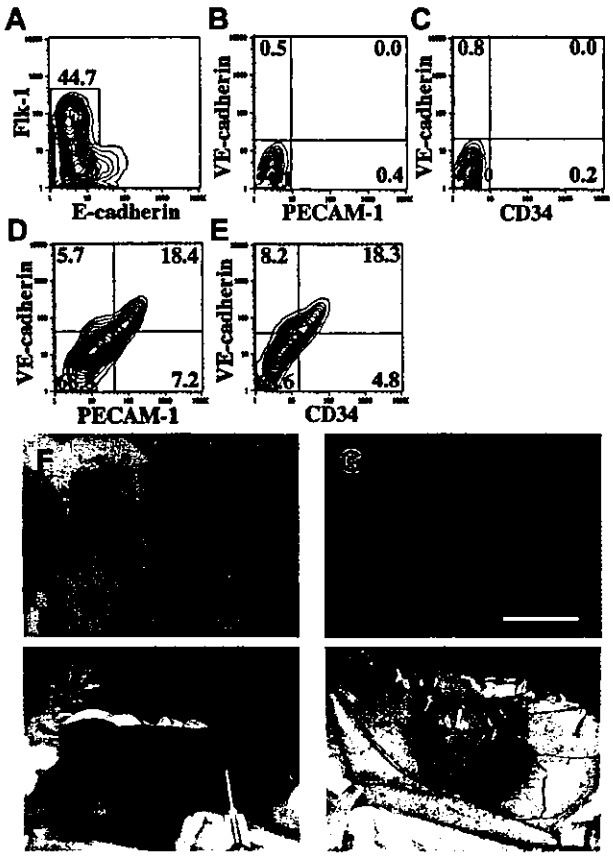

Figure 1. Characterization of injected ES cell-derived VPCs and transplantation of VPCs in tumor angiogenesis model. (A-C) Flow cytometric sorting and analysis of Flk-1$^+$ undifferentiated VPCs. ÇCE/nLacZ ES cells were cultured on type IV collagen-coated dishes in the absence of leukemia inhibitory factor (LIF). (A) After 4 days of differentiation, Flk-1$^+$ VPCs were sorted by flow cytometry (undifferentiated VPCs). (B-C) Flk-1$^+$ undifferentiated VPCs did not express other EC markers (VE-cadherin, PECAM-1, and CD34). (D-G) After a 3-day incubation of Flk-1$^+$ undifferentiated VPCs, differentiated VPCs were induced. Flow cytometric analysis revealed that about 30% were Flk-1$^+$VE-cadherin$^+$PECAM-1$^+$CD34$^+$ ECs and 70% were Flk-1$^-$VE-cadherin$^-$PECAM-1$^-$CD34$^-$ (D-E). (F-G) Double staining of differentiated VPCs was performed as previously reported.[1] About 70% of cells that lost Flk-1 expression were positive for SMA (brown) and surrounded PECAM-1$^+$ EC sheets (blue). (F) The expressions of PECAM-1 and SMA were exclusive for differentiated VPCs (scale bar, 100 μm). (G) Fluorescent immunostaining of Flk-1 (red) and SMA (green) revealed that they were expressed exclusively (scale bar 20 μm). (H-I) Tumor angiogenesis model of nude mice. Subcutaneous transplantation of VPCs to the growing tumor 7 days after C6 glioblastoma cell implantation was performed (H). Vascularized tumor was obtained 5 days after VPC implantation (I). Monoclonal antibody (MoAb) for murine E-cadherin (epithelial cadherin; ECCD2), Flk-1 (AVAS12), and vascular endothelial (VE)-cadherin (VECD1) have been described previously.[6,7] Fluorescein isothiocyanate (FITC)-conjugated MoAb for murine PECAM-1 (Mec13.3) and FITC-conjugated MoAb for CD34 (RAM34) were purchased from Pharmingen (San Diego, CA). MoAbs for SMA 1A4, CCA7 were obtained from Neo Markers (Fremont, CA) and ENZO Diagnostics (Farmingdale, NY).

Contribution of VPCs to the vascular component in tumor neoangiogenesis

Five days after subcutaneous injection, differentiated VPCs were demonstrated to form tubelike structures (Figure 2D), whereas undifferentiated VPCs mainly formed cell aggregates with little vascular stretch (Figure 2A). In undifferentiated VPC-injected tumors, many LacZ$^+$ cells were negative for PECAM-1 (Figure 2B-C), SMA, and CD45 (data not shown), suggesting that undifferentiated VPCs gave rise to cell types other than vascular cells. Lee et al[9] reported that unregulated VEGF expression in myocardium led to the formation of hemangioma.[10] As shown panels E and F of Figure 2, within the newly formed blood vessels with LacZ$^+$ VPC-derived cells, circulating LacZ$^-$ blood cells were clearly detected, indicating integration with the systemic circulation. We could not detect LacZ$^+$CD45$^+$ blood cells within the vessel lumen (data not shown). Circulating LacZ$^+$ blood cells were not detected by FACS analysis (data not shown). Implantation of VE-cadherin$^+$ endothelial fraction of differentiated VPCs also generated similar tube structures (Figure 2G) and contributed to the developing capillary network (Figure 2H-I). To investigate the impact of differentiation stages of ES cells for transplantation efficiency, we counted LacZ$^+$PECAM-1$^+$ cells that contributed to vascular structures (Figure 2M). Percentages of LacZ$^+$PECAM-1$^+$ cells to all LacZ$^+$ cells were 39.5% ± 14.1% (mean ± SEM; n = 3) in the undifferentiated VPC injection group, 86.9% ± 4.9% in the differentiated VPC group ($P < .05$ versus undifferentiated VPCs), and 95.3% ± 3.3% in the VE-cadherin$^+$ fraction injection group ($P < .05$ versus undifferentiated VPCs). In contrast, we did not detect LacZ$^+$ cells within the tumor after the intravenous administration of VPCs.

Interaction between ECs and MCs is essential for vascular development and maintenance of vascular integrity.[11,12] Because differentiated VPCs contained substantial numbers of SMA$^+$Flk-1$^-$ MCs, we examined the participation of the MC component to pericyte recruitment during tumor neoangiogenesis. LacZ$^+$SMA$^+$-PECAM-1$^-$ cells were detected in differentiated VPC-injected tumors (Figure 2N-O). In differentiated VPC transplantation, however, the ratio of LacZ$^+$SMA$^+$ cells to total LacZ$^+$ cells was much lower than that of LacZ$^+$PECAM-1$^+$ cells. To analyze the in vivo survival/proliferation potential of MCs, we performed selective induction of Flk-1$^-$SMA$^+$ cells from Flk-1$^+$ cells with PDGF-BB and transplanted them into the tumor. Whole-mount

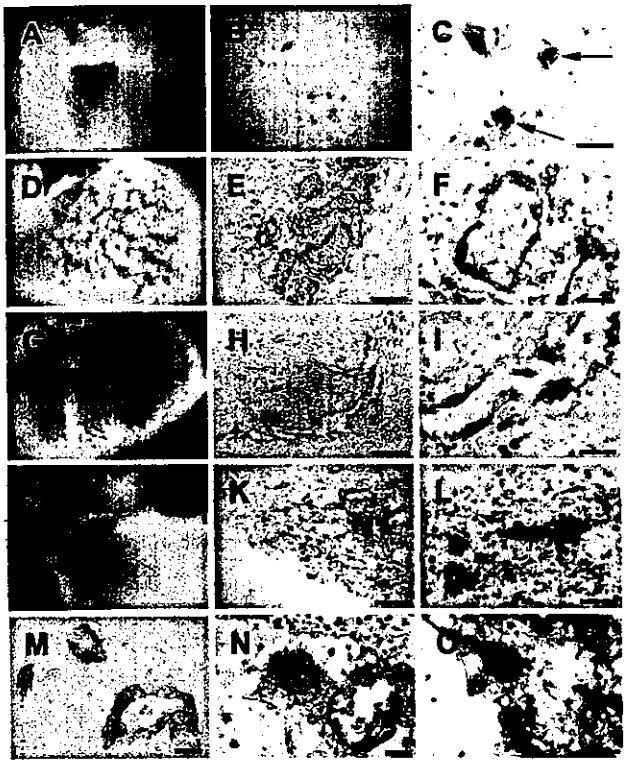

Figure 2. Contribution of ES cell-derived VPCs to tumor angiogenesis. (A,D,G,J) Whole-mount X-gal staining of the tumor. An X-gal analog, blue gal (Nacalai), was used as a substrate for staining 5 days after the injection of undifferentiated VPCs (A), differentiated VPCs (D), VE-cadherin$^+$ fraction of differentiated VPCs (G), and PDGF-BB–treated VPC (J). Undifferentiated VPCs and PDGF-BB–treated VPCs formed cell aggregates with few vascular structures (A,J). Differentiated VPCs and VE-cadherin$^+$ fraction of differentiated VPCs generated rich vascular-like networks (D,G). (B,C,E,F,H,I,K-O) Immunohistochemical staining of tumor sections. Differentiated VPCs were specifically incorporated as LacZ (blue)/PECAM-1 (brown) double-positive cells into developing vasculatures (E-F). Undifferentiated VPCs were often detected as LacZ$^+$/PECAM-1$^-$ cells (arrows; B-C). Implantation of VE-cadherin$^+$Flk-1$^+$ fraction of differentiated VPCs similarly generated specific vascular contribution as LacZ/PECAM-1 double-positive cells (H-I). Typical LacZ$^+$PECAM-1$^+$ cells (M) were observed in the differentiated VPC-injected tumor. LacZ (blue)/SMA (purple) double-positive and PECAM-1 (brown)-negative cells were also detected in the continuous sections (N-O). In the PDGF-BB–treated VPC transplantation group, some LacZ (blue)/SMA (red) double-positive cells were detected (K-L). Scale bars: panels B, E, H, K, 250 μm; panels C, F, I, L, 50 μm; panel M, 100 μm; panels N-O, 25μm.

LacZ staining of the tumor revealed that transplanted PDGF-BB–treated VPCs remained less than differentiated VPCs and formed cell aggregates (Figure 2J) similar to undifferentiated VPCs (Figure 2A). We detected some LacZ$^+$SMA$^+$ cells (Figure 2K-L) and only a few LacZ$^+$PECAM-1$^+$ cells. Most LacZ$^+$ cells were negative for either. This result indicated that although VPC-derived MCs can contribute to the MC component in tumor neoangiogenesis, the in vivo survival/proliferation potential of MCs is not high.

Transplantation of VPCs quantitatively augmented tumor blood flow in nude mice

We further investigated whether transplantation of VPCs might augment blood flow of the tumors. LDPI analyses revealed the significantly augmented ratio of differentiated VPC transplantation to control tumor blood flow (Figure 3A-B), whereas the blood flow ratios of other VPC transplantation groups were not altered. Quantification of the number of tumor blocks containing LacZ$^+$ cells demonstrated an increase of the extent of vascular expansion (Figure 3C). About 40% of tumor blocks contained LacZ$^+$ cells in the differentiated VPC transplantation group, whereas about 10% of them were seen in other VPC transplantation groups. In our protocol, no significant differences in the tumor weight were observed between control and VPC transplantation tumors among the 3 groups (data not shown).

Asahara et al[13] first demonstrated the existence of endothelial progenitor cells (EPCs) in the circulation, which are at least in part derived from bone marrow,[2] and showed that they can participate in postnatal angiogenesis after intravenous administration.[13] In our present study, intravenously administrated ES cell–derived VPCs did not contribute to tumor neoangiogenesis, suggesting that ES cell-derived VPCs might be different from somatic circulating endothelial progenitors especially in recruitment and adhesion property. EPCs were characterized as CD34$^+$Flk-1$^+$AC133$^+$ cells.[13-15] These precursors differentiated into Flk-1$^+$AC133$^-$ acetyl low-density lipoprotein (LDL) incorporated-positive ECs.[3,14-16] Our ES cell-derived VPCs are Flk-1$^+$CD34$^-$ and can differentiate into both MCs and ECs.[1] Thus, VPCs are supposed to be more premature precursors. Our results demonstrate that these undifferentiated VPCs cannot be specifically differentiated into ECs and MCs in vivo. However, differentiated VPCs, that is, VPC-derived vascular cells (ECs and MCs) at defined differentiation stages can contribute to tumor-associated vasculoangiogenesis.

The results of the present study clearly demonstrate that differentiated vascular cells derived from VPCs can contribute to generation of vascular structures in adult neoangiogenesis. Optimization of the differentiation stage of ES cells at transplantation is thus critically required to meet the challenge for cell therapy in regeneration medicine.

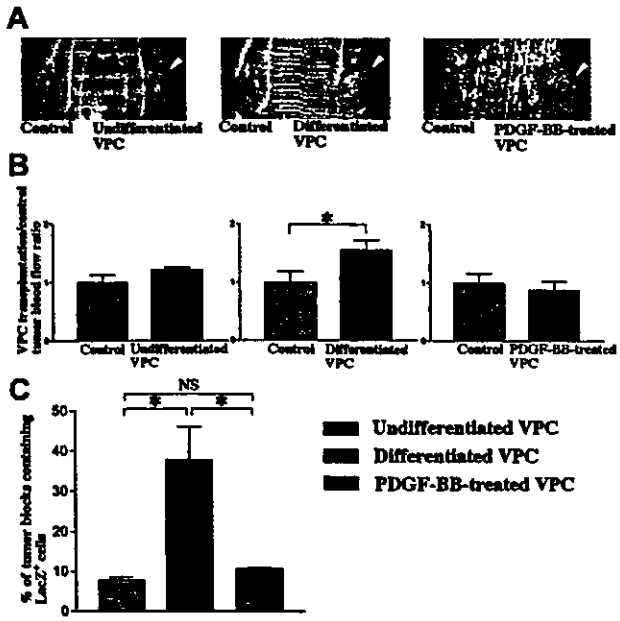

Figure 3. Augmented blood flow in tumors by subcutaneous transplantation of VPCs and expansion of transplanted VPCs within the tumor. (A) LDPI analyses of blood flow in 3 VPC transplantation groups. Bilateral generation of C6-derived tumor (black circles) and unilateral transplantation of VPCs (arrowheads) in nude mice is shown. Differentiated VPC transplantation augmented blood flow of tumor (red to white colors) compared with control, whereas undifferentiated and PDGF-BB–treated VPCs did not (blue to green colors). (B) Quantitative analyses demonstrated the significant enhancement of differentiated VPC transplantation/control tumor blood flow ratios in nude mice. Data shown (mean ± SEM) are representative of 3 experiments. *$P < .05$. (C) Percents of the number of sectioned tumor blocks containing LacZ$^+$ cells. About 40% of tumor blocks contained LacZ$^+$ cells in differentiated VPC transplantation groups, whereas about 10% of them did in other VPC transplantation groups. The number of tumor blocks containing LacZ$^+$ cells in differentiated VPC transplantation groups was significantly increased. Data shown (mean ± SEM) are representative of 3 experiments. *$P < .01$; NS, $P > .05$.

References

1. Yamashita J, Itoh H, Hirashima M, et al. Flk1-positive cells derived from embryonic stem cells serve as vascular progenitors. Nature. 2000;408: 92-96.
2. Asahara T, Takahashi T, Masuda H, et al. VEGF contributes to postnatal neovascularization by mobilizing bone marrow-derived endothelial progenitor cells. EMBO J. 1999;18:3964-3972.
3. Murohara T, Ikeda H, Duan J, et al. Transplanted cord blood-derived endothelial precursor cells augment postnatal neovascularization. J Clin Invest. 2000;105:1527-1536.
4. Kalka C, Masuda H, Takahashi T, et al. Transplantation of ex vivo expanded endothelial progenitor cells for therapeutic neovascularization. Proc Natl Acad Sci U S A. 2000;97:3422-3427.
5. Robertson E, Bradley A, Kuehn M, Evans M. Germ-like transmission of genes introduced into cultured pluripotential cells by retroviral vector. Nature. 1986;323:445-448.
6. Nishikawa SI, Nishikawa S, Hirashima M, Matsuyoshi N, Kodama H. Progressive lineage analysis by cell sorting and culture identifies Flk-1$^+$ VE-cadherin$^+$ cells at a diverging point of endothelial and hemopoietic lineages. Development.1998;125:1747-1757.
7. Hirashima M, Kataoka H, Nishikawa S, Matsuyoshi N, Nishikawa SI. Maturation of embryonic stem cells into endothelial cells in an in vitro model of vasculogenesis. Blood. 1999;93:1253-1263.
8. Kubo H, Fujiwara T, Jussila L, et al. Involvement of vascular endothelial growth factor receptor-3 in maintenance of integrity of endothelial cell lining during tumor angiogenesis. Blood. 2000;96:546-553.
9. Lee RJ, Springer ML, Blanco-Bose WE, Shaw R, Ursell PC, Blau HM. VEGF gene delivery to myocardium. Deleterious effects of unregulated expression. Circulation. 2000;102:898-901.
10. Carmeliet P. VEGF gene therapy: stimulating angiogenesis or angioma-genesis? Nat Med. 2000; 6:1102-1103.
11. Carmeliet P. Mechanisms of angiogenesis and arteriogenesis. Nat Med. 2000;6:389-395.
12. Pettersson A, Nagy JA, Brown LF, et al. Heterogeneity of angiogenic response induced in different normal adult tissues by vascular permeability factor/vascular endothelial growth factor. Lab Invest. 2000;80:99-115.
13. Asahara T, Murohara T, Sullivan A, et al. Isolation of putative progenitor endothelial cells for angiogenesis. Science. 1997;275:964-966.
14. Gehling UM, Ergun S, Schumacher U, et al. In vitro differentiation of endothelial cells from AC133-positive progenitor cells. Blood. 2000;95: 3106-3112.
15. Peichev M, Naiyer AJ, Pereira D, et al. Expression of VEGFR-2 and AC133 by circulating human CD34 (+) cells identifies a population of functional endothelial precursors. Blood.2000;95: 952-958.
16. Lin Y, Weisdorf DJ, Solovey A, Hebbel RP. Origins of circulating endothelial cells and endothelial outgrowth from blood. J Clin Invest. 2000;105: 71-77.

The EMBO Journal Vol. 22 No. 23 pp. 6310–6321, 2003

NRSF regulates the fetal cardiac gene program and maintains normal cardiac structure and function

Koichiro Kuwahara, Yoshihiko Saito[1,2], Makoto Takano[3], Yuji Arai[4], Shinji Yasuno, Yasuaki Nakagawa, Nobuki Takahashi, Yuichiro Adachi, Genzo Takemura[5], Minoru Horie[6], Yoshihiro Miyamoto[7], Takayuki Morisaki[4], Shinobu Kuratomi[3], Akinori Noma[3], Hisayoshi Fujiwara[5], Yasunao Yoshimasa[7], Hideyuki Kinoshita, Rika Kawakami, Ichiro Kishimoto, Michio Nakanishi, Satoru Usami, Yoshitomo Saito, Masaki Harada and Kazuwa Nakao

Department of Medicine and Clinical Science and [6]Department of Cardiovascular Medicine, Kyoto University Graduate School of Medicine, Kyoto 606-8507, [3]Department of Physiology and Biophysics, Kyoto University Graduate School of Medicine, Kyoto 606-8501, [4]Department of Bioscience, National Cardiovascular Center Research Institute, [7]Division of Atherosclerosis and Diabetes Mellitus, National Cardiovascular Center, Suita, Osaka 565-8565 and [5]Department of Second Internal Medicine, Gifu University, Gifu 500-8705, Japan

[1]Present address: 1st Department of Internal Medicine, Nara Medical University, 840 Shijo-cho Kashihara-city Nara, 634-8522, Japan

[2]Corresponding author
e-mail: yssaito@nmu-gw.naramed-u.ac.jp

Reactivation of the fetal cardiac gene program is a characteristic feature of hypertrophied and failing hearts that correlates with impaired cardiac function and poor prognosis. However, the mechanism governing the reversible expression of fetal cardiac genes remains unresolved. Here we show that neuron-restrictive silencer factor (NRSF), a transcriptional repressor, selectively regulates expression of multiple fetal cardiac genes, including those for atrial natriuretic peptide, brain natriuretic peptide and α-skeletal actin, and plays a role in molecular pathways leading to the re-expression of those genes in ventricular myocytes. Moreover, transgenic mice expressing a dominant-negative mutant of NRSF in their hearts exhibit dilated cardiomyopathy, high susceptibility to arrhythmias and sudden death. We demonstrate that genes encoding two ion channels that carry the fetal cardiac currents I_f and $I_{Ca,T}$, which are induced in these mice and are potentially responsible for both the cardiac dysfunction and the arrhythmogenesis, are regulated by NRSF. Our results indicate NRSF to be a key transcriptional regulator of the fetal cardiac gene program and suggest an important role for NRSF in maintaining normal cardiac structure and function.
Keywords: arrhythmia/cardiomyopathy/fetal cardiac genes/transcription

Introduction

Cardiac hypertrophy is initially an adaptive response of the heart to mechanical stress, tissue injury or neurohumoral activation; however, sustained hypertrophy can lead to dilated cardiomyopathy and heart failure. Up to 50% of the deaths among heart failure patients are sudden and unexpected, and are presumably the result of lethal arrhythmias (Tomaselli and Marbán, 1999). The dysregulation of a panel of cardiac genes accounts for the biochemical, structural, functional and electrical alterations in failing hearts, but relatively little is known about the molecular pathways underlying those complex remodeling processes. One of the characteristic genetic alterations in hypertrophied and failing hearts is reactivation of a fetal cardiac gene program, i.e. upregulation of genes encoding atrial and brain natriuretic peptides (ANP and BNP, respectively), as well as fetal contractile protein isoforms such as β-myosin heavy chain (MHC) and α-skeletal actin (Chien *et al.*, 1991). Indeed, production of ANP and BNP in cardiomyocytes is markedly augmented in hypertrophied and failing hearts and is a prognostic indicator of clinical severity (Kjær and Hesse, 2001). Accordingly, elucidation of the regulatory mechanisms governing expression of these fetal cardiac genes should enable one to understand better the processes by which cardiac hypertrophy and heart failure are established.

Altered expression of certain ion channels in diseased hearts is also indicative of the reactivation of a fetal gene program. Two ionic currents, the hyperpolarization activated non-selective cation current (I_f) and the T-type Ca^{2+} current ($I_{Ca,T}$), which are normally expressed in fetal ventricles but repressed in adult ventricles, are re-expressed in ventricular myocytes of hypertrophied or failing hearts, perhaps increasing the vulnerability of the hearts to ventricular arrhythmias (Nuss and Houser, 1993; Sen and Smith, 1994; Cerbai *et al.*, 1996, 2001; Martinez *et al.*, 1999). Moreover, increased expression of $I_{Ca,T}$ might contribute to the progression of heart failure (Clozel *et al.*, 1999). Thus, elucidation of the mechanisms that control the fetal cardiac gene program may also shed light on the molecular basis for arrhythmias and sudden death associated with heart failure.

Despite considerable effort, virtually the entire process by which reversible expression of fetal cardiac genes is governed remains unknown. It was shown recently that (i) a repressor element named neuron-restrictive silencer element (NRSE), also known as repressor element-1 (RE-1) (Kraner *et al.*, 1992; Mori *et al.*, 1992), is present in the 3′-untranslated region (UTR) of *ANP*; (ii) NRSE represses basal expression of *ANP* in ventricular myocytes by recruiting the transcriptional repressor neuron-restrictive silencer factor (NRSF), also known as RE-1 silencing transcription factor (REST) (Schoenherr and Anderson, 1995; Chong *et al.*, 1995), which forms a complex with

histone deacetylases (HDACs); and (iii) attenuation of NRSE-mediated repression is an important component of the signaling pathways by which endothelin (ET)-1 induces *ANP* promoter activity (Kuwahara *et al.*, 2001). We also showed that NRSE in the 5′-flanking region of *BNP* represses transcription of *BNP* and that attenuation of NRSE-mediated repression contributes to the increase in *BNP* transcription induced by hypertrophic stimuli (Ogawa *et al.*, 2002). Notably, NRSE is also reportedly present in the α-skeletal actin gene (Schoenherr *et al.*, 1996).

The aforementioned findings suggest that the NRSE–NRSF system regulates the expression of multiple fetal cardiac genes. However, the role of the NRSE–NRSF system in the expression of endogenous fetal cardiac genes and in the regulation of cardiac function remains unknown. To address these questions, in this study, we used a recombinant adenovirus expressing a dominant-negative mutant of NRSF (dnNRSF) and transgenic mice expressing dnNRSF in their hearts. We show that the inhibition of NRSF induces endogenous expression of multiple fetal cardiac genes in ventricular myocytes and markedly reduces the response of fetal cardiac genes to hypertrophic stimuli both *in vitro* and *in vivo*, suggesting that NRSF-mediated repression contributes to the dynamic regulation of expression of fetal cardiac genes, and that persistent inhibition of cardiac NRSF repressor function leads to dilated cardiomyopathy and sudden death. We also show that the genes encoding the ion channels that carry I_f and $I_{Ca,T}$ are upregulated in the ventricles of the transgenic mice, and that they are downstream targets of NRSF. Taken together, our findings indicate that NRSF is a novel and important regulator of the fetal cardiac gene program responsible for maintaining normal cardiac structure and function, and that NRSF plays a key role in mediating signaling pathways that lead to heart failure and sudden cardiac death.

Results

NRSF regulates endogenous cardiac fetal gene expression in vitro and in vivo

We previously used promoter–reporter constructs to show that the NRSF–NRSE system represses transcription of *ANP* and *BNP* in cultured ventricular myocytes. Moreover, the fact that NRSE is also present in the α-skeletal actin gene suggests that NRSF represses expression of multiple fetal cardiac genes (Schoenherr *et al.*, 1996; Kuwahara *et al.*, 2001; Ogawa *et al.*, 2002). To confirm the function of NRSF in the regulation of endogenous fetal cardiac gene expression, we infected cultured ventricular myocytes with a recombinant adenovirus expressing dnNRSF (Ad/dnNRSF) and examined the resultant gene expression. dnNRSF contains a DNA-binding domain but lacks two identified repressor domains, and thus inhibits NRSE-mediated repression (Chen *et al.*, 1998). We previously confirmed that this dnNRSF construct removes the repression of NRSE-containing reporter constructs exclusively in cultured ventricular myocytes (Kuwahara *et al.*, 2001; Ogawa *et al.*, 2002). Endogenous expression of *ANP*, *BNP* and *α-skeletal actin* mRNA, but not *α-cardiac actin* or *GAPDH* mRNA was markedly increased in ventricular

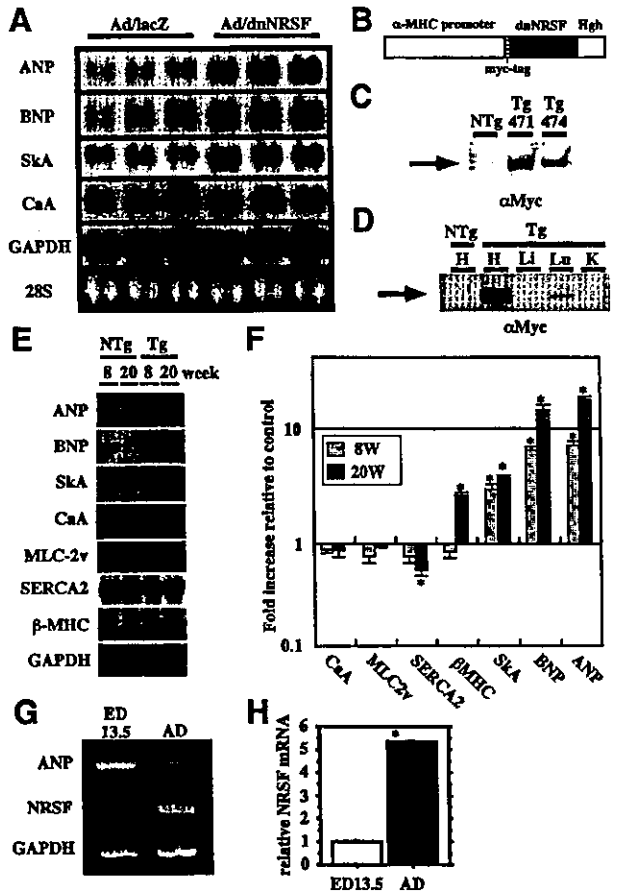

Fig. 1. NRSF regulates expression of endogenous ANP, BNP and α-skeletal actin in ventricular myocytes. (A) Northern blots showing levels of *ANP*, *BNP*, *α-skeletal actin* (*SkA*), *α-cardiac actin* (*CaA*) and *GAPDH* mRNA in cultured ventricular myocytes infected with Ad/lacZ or Ad/dnNRSF for 24 h. (B) A cDNA construct for the generation of dnNRSF Tg mice; Hgh, the poly(A) sequence of human growth hormone gene. (C) Western blot analysis for dnNRSF expression in ventricles from NTg and two different founders lines of dnNRSF Tg mice (Tg471 and 474). (D) Western blot analysis for dnNRSF expression in various organs from dnNRSF Tg mice: H, heart; Lu, lung; L, liver; K, kidney. (E) Representative northern blots showing levels of the indicated mRNAs in dnNRSF Tg and NTg hearts. (F) Bar graph summarizing the relative cardiac levels of the indicated mRNAs (normalized to *GAPDH* mRNA levels) detected in the northern blots shown in (E); bars represent means ± SEM from three independent experiments; $*P < 0.05$ versus NTg hearts; $n = 6$ each. (G) RT–PCR analysis for *NRSF* and *ANP* mRNA expression in ventricles from 13.5-day mouse embryos (ED 13.5) and 20-week-old adult mice (AD). (H) Bar graphs showing relative *NRSF* mRNA levels (normalized to *GAPDH* mRNA levels) determined by quantitative RT–PCR. Bars represent means ± SEM from three independent assays; $*P < 0.05$ versus ED13.5.

myocytes infected with Ad/dnNRSF, as compared with cells infected with control vector (Figure 1A).

Because mice lacking *NRSF* die *in utero*, it is impossible to use these animals to analyze NRSF function in the post-natal heart (Chen *et al.*, 1998). However, expression of dnNRSF in chick embryo using a retroviral vector caused ectopic expression of a specific set of neuronal genes, as did targeted deletion of *NRSF* in mice (Chen *et al.*, 1998). Therefore, to investigate the role of NRSF in the post-natal heart, we produced transgenic mice that express dnNRSF under the control of the cardiac-specific